

Mechanism of Lithium Diisopropylamide-Mediated Ortholithiation of
1,4-bis(Trifluoromethyl)benzene under Nonequilibrium Conditions:
Condition-Dependent Rate Limitation
and
Lithium Chloride-Catalyzed Inhibition

Jun Liang, Alexander C. Hoepker, Russell F. Algera, Yun Ma,
and David B. Collum*

Contribution from the Department of Chemistry and Chemical Biology
Baker Laboratory, Cornell University, Ithaca, New York 14853-1301

Part 1: Experimental Procedures	S7

Part 2: NMR Spectroscopic Studies	S8

Figure 1. ^{19}F NMR spectrum of LDA (0.10 M) with 1 (0.050 M) in 12.2 M THF after aging for 10 minutes at $-78\text{ }^\circ\text{C}$.	S8
Figure 2. ^6Li NMR spectrum of $[^6\text{Li},^{15}\text{N}]\text{LDA}$ (0.10 M) and 1 (0.050 M) in 12.2 M THF recorded at $-78\text{ }^\circ\text{C}$.	S8
Figure 3. $^{13}\text{C}\{^1\text{H}\}$ NMR spectrum of 2 generated from 1 (0.15 M) with $[^6\text{Li}]\text{LDA}$ (0.30 M, 2.0 equiv) in 12.2 M THF- d_8 at $-100\text{ }^\circ\text{C}$.	S9
Figure 4. $^{13}\text{C}\{^{19}\text{F}\}$ NMR spectrum of 2 generated from 1 (0.15 M) with $[^6\text{Li}]\text{LDA}$ (0.30 M, 2.0 equiv) in 12.2 M THF- d_8 at $-100\text{ }^\circ\text{C}$.	S10
Figure 5. $^{13}\text{C}\{^{19}\text{F}\}$ NMR spectrum of 2-d_3 generated from 1-d_4 (0.15 M) with $[^6\text{Li}]\text{LDA}$ (0.30 M) in 12.2 M THF- d_8 at $-100\text{ }^\circ\text{C}$.	S11
Figure 6. Plot of $\{[i\text{-Pr}_2\text{NH}][\text{ArLi}]\} / \{[\text{LDA}]^{(1/2)}[\text{ArH}]\}$ vs $[\text{THF}]$ for the ortholithiation of 1 (0.005 M) with LDA (0.10 M) and diisopropylamine (0.025 M) at $-78\text{ }^\circ\text{C}$.	S12
Part 3: Rate Studies	S13

Figure 7. Representative in situ IR traces for the ortholithiation of 1 (0.005 M) by LDA (0.10 M) in THF at $-78\text{ }^\circ\text{C}$.	S13

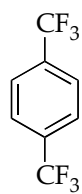
Figure 8. Ortholithiation of 1 (0.09 M) with LDA (0.10 M) in 12.2 M THF at $-78\text{ }^{\circ}\text{C}$ with injection of 1.0 mol % LiCl.	S14
Figure 9. Representative plot showing concentration of arene 1 vs time for the ortholithiation of 1 (0.005 M) with LDA (0.10 M) in 12.2 M THF at $-78\text{ }^{\circ}\text{C}$.	S14
Figure 10. Representative plot showing poor exponential fit to the decay of ortholithiation of 1 (0.005 M) with LDA (0.10 M) in THF (12.2 M) at $-78\text{ }^{\circ}\text{C}$.	S15
Figure 11. Competitive ortholithiation of 1 (0.005 M) and 1-<i>d</i>₄ (0.005 M) with LDA (0.10 M) in THF (12.2 M) at $-78\text{ }^{\circ}\text{C}$.	S16
Figure 12. Competitive ortholithiation of 1 (0.005 M) and 1-<i>d</i>₄ (0.005 M) with LDA (0.10 M) in the presence of 1 mol % LiCl in THF (12.2 M) at $-78\text{ }^{\circ}\text{C}$.	S16
Figure 13. Ortholithiation of 1-<i>d</i>₃ (0.032 M) with LDA (0.10 M) in 12.2 M <i>d</i> ₈ -THF monitored by ^1H NMR.	S17
Figure 14. Plot of initial rate vs [ArH] for the ortholithiation of 1 with LDA (0.050 M) in THF (12.2 M) at $-78\text{ }^{\circ}\text{C}$.	S18
Figure 15. Plot of initial rate vs [ArH] for the ortholithiation of 1 with LDA (0.20 M) in THF (3.05 M) at $-78\text{ }^{\circ}\text{C}$.	S19
Figure 16. Plot of initial rate versus [LDA] in THF (3.05 M) for the ortholithiation of 1 (0.005 M) at $-78\text{ }^{\circ}\text{C}$.	S20
Figure 17. Plot of initial rate versus [LDA] in THF (6.10 M) for the ortholithiation of 1 (0.005 M) at $-78\text{ }^{\circ}\text{C}$.	S21
Figure 18. Plot of initial rate versus [LDA] in THF (9.15 M) for the ortholithiation of 1 (0.005 M) at $-78\text{ }^{\circ}\text{C}$.	S22
Figure 19. Plot of initial rate versus [LDA] in THF (12.2 M) for the ortholithiation of 1 (0.005 M) at $-78\text{ }^{\circ}\text{C}$.	S23
Figure 20. Plot of initial rate versus [THF] in hexanes for the ortholithiation of 1 (0.005 M) by LDA (0.050 M) at $-78\text{ }^{\circ}\text{C}$.	S24
Figure 21. Plot of initial rate versus [THF] in hexanes for the ortholithiation of 1 (0.005 M) by LDA (0.10 M) at $-78\text{ }^{\circ}\text{C}$.	S25
Figure 22. Plot of initial rate versus [THF] in hexanes for the ortholithiation of 1 (0.005 M) by LDA (0.15 M) at $-78\text{ }^{\circ}\text{C}$.	S26

Figure 23. Plot of initial rate versus [THF] in hexanes for the ortholithiation of 1 (0.005 M) by LDA (0.20 M) at $-78\text{ }^{\circ}\text{C}$.	S27
Figure 24. Plot of initial rate versus [LDA] in THF (12.2 M) for the ortholithiation of 1 (0.060 M) at $-78\text{ }^{\circ}\text{C}$.	S28
Figure 25. Plot of initial rate versus [THF] in hexanes for the ortholithiation of 1 (0.005 M) by LDA (0.20 M) at $-78\text{ }^{\circ}\text{C}$.	S29
Figure 26. Plot of initial rate versus [LiCl] for the ortholithiation of 1 (0.05 M) by 0.10 M LDA in 12.2 M THF at $-78\text{ }^{\circ}\text{C}$.	S30
Figure 27. Plot of initial rate vs [ArH] for the ortholithiation of 1 with LDA (0.10 M) in THF (12.2 M) with 1.0 mol% LiCl at $-78\text{ }^{\circ}\text{C}$.	S31
Figure 28. Plot of initial rate versus [LDA] in THF (12.2 M) for the ortholithiation of 1 (0.050 M) in the presence of 1.0 mol% LiCl at $-78\text{ }^{\circ}\text{C}$.	S32
Figure 29. Plot of initial rate versus [THF] in Et ₂ O and in hexanes cosolvent for the ortholithiation of 1 (0.05 M) by LDA (0.10 M) in the presence of 1.0 mol% LiCl at $-78\text{ }^{\circ}\text{C}$.	S33
Figure 30. Plot of initial rate vs [ArD ₄] for the ortholithiation of 1-d₄ with LDA (0.10 M) in THF (12.2 M) at $-42\text{ }^{\circ}\text{C}$.	S34
Figure 31. Plot of initial rate versus [LDA] in THF (12.2 M) for the ortholithiation of 1-d₄ (0.005 M) at $-42\text{ }^{\circ}\text{C}$.	S35
Figure 32. Plot of initial rate versus [THF] in Et ₂ O cosolvent for the ortholithiation of 1-d₄ (0.005 M) by LDA (0.10 M) at $-42\text{ }^{\circ}\text{C}$.	S36
Figure 33. Plot of initial rate versus [LiCl] for the ortholithiation of 1-d₄ (0.005 M) by 0.30 M LDA in 12.2 M THF at $-42\text{ }^{\circ}\text{C}$.	S37
Figure 34. Plot of initial rate versus [ArD ₄] for the ortholithiation of 1-d₄ (0.005 M) by LDA (0.10 M) in the presence of 3.0 mol% LiCl at $-42\text{ }^{\circ}\text{C}$.	S38
Figure 35. Plot of initial rate versus [LDA] in THF (12.2 M) for the ortholithiation of 1-d₄ (0.005 M) in the presence of 3.0 mol% LiCl at $-42\text{ }^{\circ}\text{C}$.	S39
Figure 36. Plot of initial rate versus [THF] in Et ₂ O cosolvent for the ortholithiation of 1-d₄ (0.005 M) by LDA (0.10 M) in the presence of 3.0 mol% LiCl at $-42\text{ }^{\circ}\text{C}$.	S40
Figure 37. Plot of initial rate vs [ArD ₄] for the ortholithiation of 1-d₄ with LDA (0.10 M) in THF (12.2 M) with at $-78\text{ }^{\circ}\text{C}$.	S41

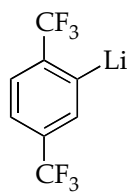
Figure 38. Plot of initial rate versus [LDA] in THF (12.2 M) for the ortholithiation of 1-d₄ (0.005 M) at -78 °C.	S42
Figure 39. Plot of initial rate versus [LDA] in THF (3.05 M) for the ortholithiation of 1-d₄ (0.005 M) at -78 °C.	S43
Figure 40. Plot of initial rate versus [THF] in hexanes for the ortholithiation of 1-d₄ (0.005 M) by LDA (0.10 M) at -78 °C.	S44
Figure 41. Plot of initial rate versus [THF] in hexanes for the ortholithiation of 1-d₄ (0.005 M) by LDA (0.050 M) at -78 °C.	S45
Figure 42. Plot of initial rate versus [THF] in hexanes for the ortholithiation of 1-d₄ (0.005 M) by LDA (0.20 M) at -78 °C.	S46
Figure 43. Plot of initial rate versus [LiCl] for the ortholithiation of 1-d₄ (0.005 M) by 0.10 M LDA in 12.2 M THF at -78 °C.	S47
Figure 44. Plot of initial rate versus [ArD ₄] for the ortholithiation of 1-d₄ (0.005 M) by LDA (0.10 M) in the presence of 2.0 mol% LiCl at -78 °C.	S48
Figure 45. Plot of initial rate versus [LDA] in THF (12.2 M) for the ortholithiation of 1-d₄ (0.005 M) in the presence of 2.0 mol% LiCl at -78 °C.	S49
Figure 46. Plot of initial rate versus [THF] in Et ₂ O for the ortholithiation of 1-d₄ (0.005 M) by LDA (0.10 M) in the presence of 2.0 mol% LiCl at -78 °C.	S50
Figure 47. Plot of initial rate versus [LiCl] for the ortholithiation of 1-d₄ (0.005 M) by 0.10 M LDA in 12.2 M THF at -90 °C.	S51
Figure 48. Plot of ln(k/T) versus (1/T) for the ortholithiation of 1-d₄ (0.005 M) by LDA (0.10 M) in THF (12.2 M) at various temperatures.	S52
Scheme 1. Scheme of dimer- and monomer-based lithiations	S53
Figure 49. Simulation for the plots of initial rate vs [LDA] and monomer [A] vs catalyst concentration showing catalytic inhibition.	S54
Figure 50. Simulation for the plots of initial rate vs [LDA] and monomer [A] vs catalyst concentration showing no changes in rate.	S54
Figure 51. Simulation for the plots of initial rate vs [LDA] and monomer [A] vs catalyst concentration showing catalytic acceleration.	S55

Part 4: Derivations	S56
<hr/>	
Derivation 1. Derivation of steady-state rate expressions	S56
Part 5: Computational Studies	S59
<hr/>	
Table 1. Optimized geometries at B3LYP level of theory with 6-31G(d) basis set for the reactants at $-78\text{ }^{\circ}\text{C}$ with free energies (Hartrees) and cartesian coordinates (X, Y, Z).	S60
Table 2. Optimized geometries at B3LYP level of theory with 6-31G(d) basis set for the serial solvation of C and D at $-78\text{ }^{\circ}\text{C}$ with free energies (Hartrees) and cartesian coordinates (X, Y, Z).	S63
Table 3. Optimized geometries of trisolvated LDA open dimer transition state structures at B3LYP level of theory with 6-31G(d) basis set for the ortholithiation of 1 at $-78\text{ }^{\circ}\text{C}$ with free energies (Hartrees), and cartesian coordinates (X,Y,Z).	S65
Table 4. Optimized geometries of monomer-based transition state structures at B3LYP level of theory with 6-31G(d) basis set for the ortholithiation of 1 at $-78\text{ }^{\circ}\text{C}$ with free energies (Hartrees), and cartesian coordinates (X,Y,Z).	S67
Table 5. Optimized geometries of dimer-based transition state structures at B3LYP level of theory with 6-31G(d) basis set for the ortholithiation of 1 at $-78\text{ }^{\circ}\text{C}$ with free energies (Hartrees), and cartesian coordinates (X,Y,Z).	S70
References	S75

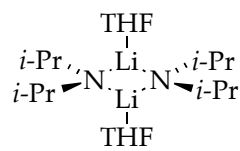
Chart 1



1



2



3

Part 1: Experimental Procedures:

2,3,5,6-Deutero-1,4-Bis(trifluoromethyl)benzene (1-*d*₄) A 10.6 M solution of *n*-BuLi in hexane (4.70 mL, 50.0 mmol) was added via syringe pump to a solution of 1,4-bis(trifluoromethyl)benzene (7.0 mL, 45.2 mmol) in 150 mL of dry THF at -78 °C under Argon over a period of 20 min. The solution was stirred for an additional 25 min. MeOD (2.03 mL, 50.0 mmol) was added via syringe pump over a period of 20 min. The mixture was allowed to stir for 1 hr. The process of sequential addition of 1.1 equiv *n*-BuLi and 1.1 equiv *d*-MeOH was repeated 5 more times. A final aliquot of MeOD (10 mL, 5.0 equiv) was added to fully quench the reaction. After the mixture was allowed to warm to room temperature, the pH was adjusted to 1.0 with 4.0 M aq HCl to dissolve all lithium salts. Organic and aqueous layers were separated, and the organic layer was extracted with more cold 0.2 M HCl to remove excess THF. Extraction was stopped when the total organic volume was approximately 10-15 mL. The organic layer was dried over Na₂SO₄ and distilled. The product was collected by distillation at 116 °C as a colorless liquid (2.26 g, 10.4 mmol) in 23% yield. ¹³C NMR δ 134.20 (q, ²J_{C-F} = 33.2 Hz), 125.75 (tq, ¹J_{C-D} = 25.5 Hz, ³J_{C-F} = 3.3 Hz), 123.80 (q, ¹J_{C-F} = 272.1 Hz); LRMS: 218.2 *m/z*.

Part 2: NMR Spectroscopic Studies

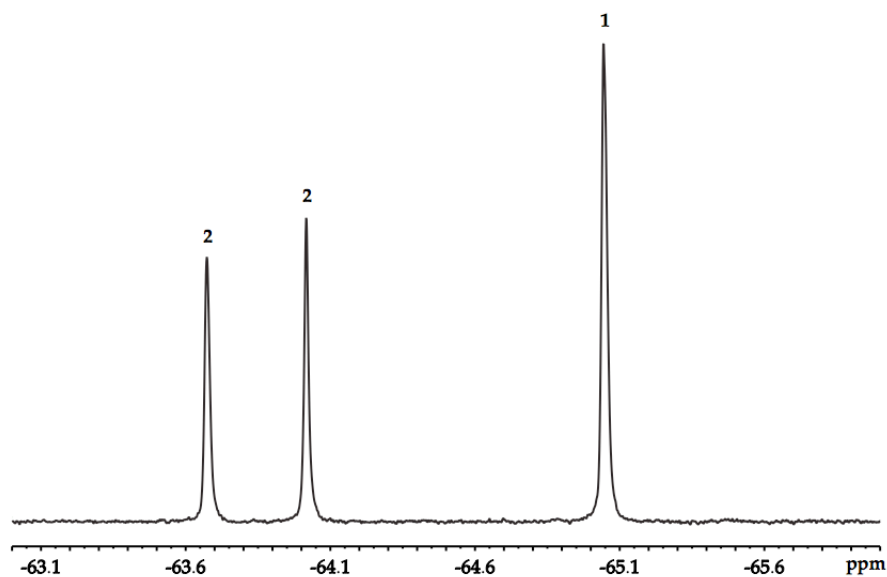


Figure 1. ^{19}F NMR spectrum of LDA (0.10 M) with **1** (0.005 M) in 12.2 M THF after aging for 10 min at $-78\text{ }^\circ\text{C}$: δ -65.05 (s), -64.02 (s), -63.67 (s).

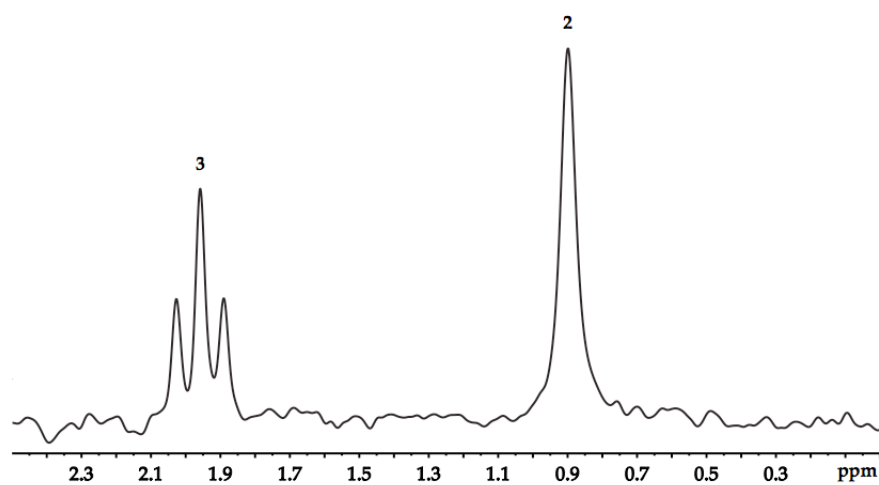


Figure 2. ^6Li NMR Spectrum of $[^6\text{Li}, ^{15}\text{N}]$ LDA (0.10 M) and **1** (0.05 M) in 12.2 M THF recorded at $-78\text{ }^\circ\text{C}$: δ 1.96 (t, $^1J_{\text{Li-N}} = 5.0\text{ Hz}$), 0.90 (s).

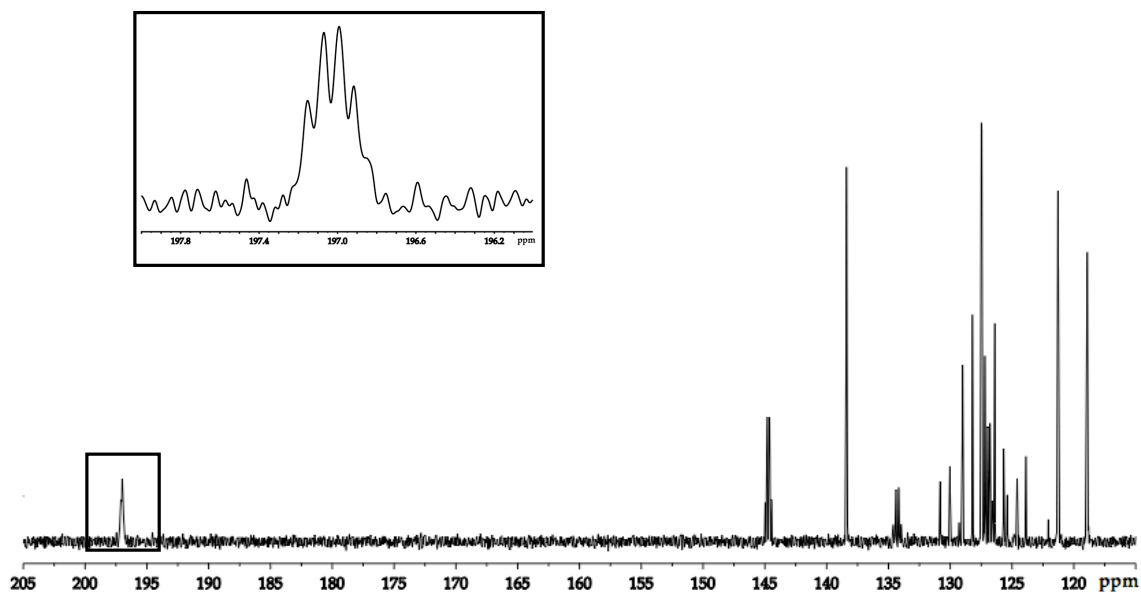


Figure 3. $^{13}\text{C}\{^1\text{H}\}$ NMR spectrum of **2** generated from **1** (0.15 M) with $[\text{}^6\text{Li}]\text{LDA}$ (0.30 M, 2.0 equiv) in 12.2 M $\text{THF-}d_8$ at $-100\text{ }^\circ\text{C}$. Resonances of **1** remain at equilibrium. **2**: δ 197.02 (m), 144.72 (q, $^2J_{\text{C-F}} = 25.2\text{ Hz}$), 138.40 (s), 128.11 (q, $^1J_{\text{C-F}} = 273.3\text{ Hz}$), 127.31 (q, $^1J_{\text{C-F}} = 273.0\text{ Hz}$), 126.88 (q, $^2J_{\text{C-F}} = 28.5\text{ Hz}$), 121.29 (s), 118.93 (s). **1**: δ 134.28 (q, $^2J_{\text{C-F}} = 32.8\text{ Hz}$), 127.48 (s), 124.79 (q, $^1J_{\text{C-F}} = 272.3\text{ Hz}$).

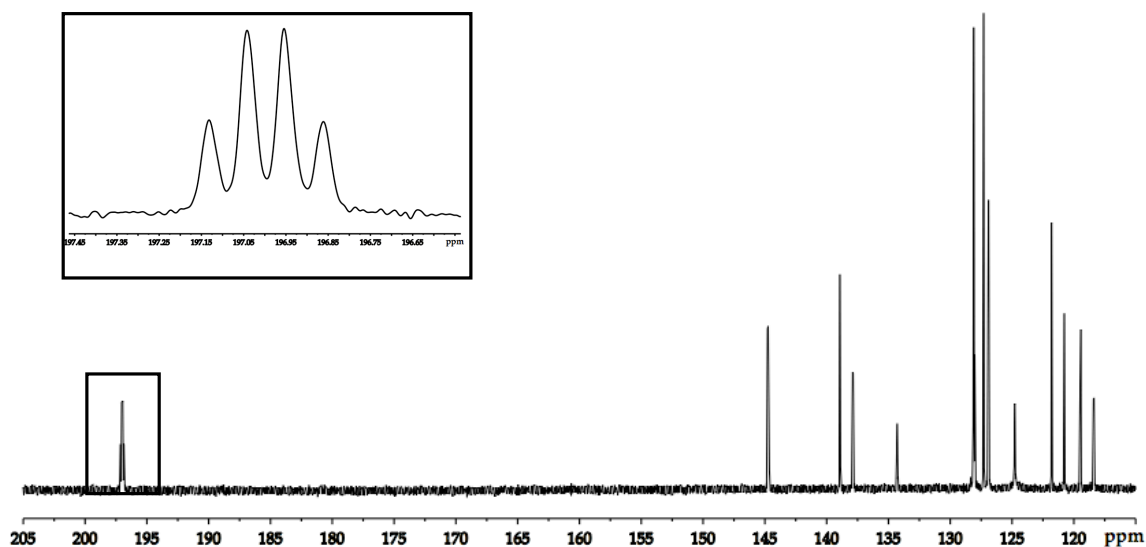


Figure 4. $^{13}\text{C}\{^{19}\text{F}\}$ NMR spectrum of **2** generated from **1** (0.15 M) with $[\text{}^6\text{Li}]\text{LDA}$ (0.30 M, 2.0 equiv) in 12.2 M $\text{THF-}d_8$ at $-100\text{ }^\circ\text{C}$. Resonances of **1** remain at equilibrium. **2**: δ 197.00 (td, $^1J_{\text{C-Li}} = 13.2\text{ Hz}$, $^2J_{\text{C-H}} = 6.6\text{ Hz}$), 144.72 (dd, $^2J_{\text{C-H}} = 12.6\text{ Hz}$, $^3J_{\text{C-H}} = 7.2\text{ Hz}$), 138.40 (dd, $^1J_{\text{C-H}} = 156.5\text{ Hz}$, $^2J_{\text{C-H}} = 5.3\text{ Hz}$), 128.11 (m), 127.31 (t, $^2J_{\text{C-H}} = 3.8\text{ Hz}$), 126.88 (m), 121.29 (d, $^1J_{\text{C-H}} = 155.3\text{ Hz}$), 118.93 (dd, $^1J_{\text{C-H}} = 160.2\text{ Hz}$, $^2J_{\text{C-H}} = 5.8\text{ Hz}$). **1**: δ 134.29 (m), 127.47 (dm, $^1J_{\text{C-H}} = 168.0\text{ Hz}$), 124.79 (m).

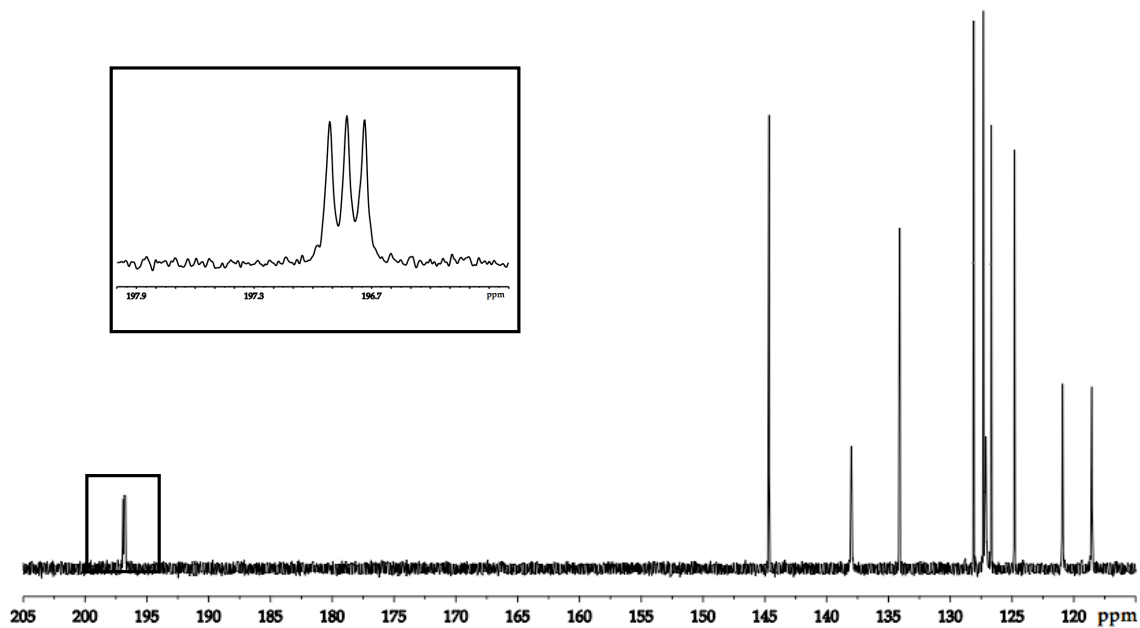


Figure 5. $^{13}\text{C}\{^{19}\text{F}\}$ NMR spectrum of $2-d_3$ generated from $1-d_4$ (0.15 M) with $[\text{}^6\text{Li}]\text{LDA}$ (0.30 M) in 12.2 M $\text{THF-}d_8$ at $-100\text{ }^\circ\text{C}$. Resonances of $1-d_4$ remain at equilibrium. $2-d_3$: δ 196.83 (t, $^1J_{\text{C-Li}} = 13.2\text{ Hz}$) 144.66 (s), 138.00 (s), 128.11 (s), 127.12 (s), 126.68 (s), 120.92 (s), 118.55 (s). $1-d_4$: δ 134.10 (s), 127.33 (s), 124.80 (s).

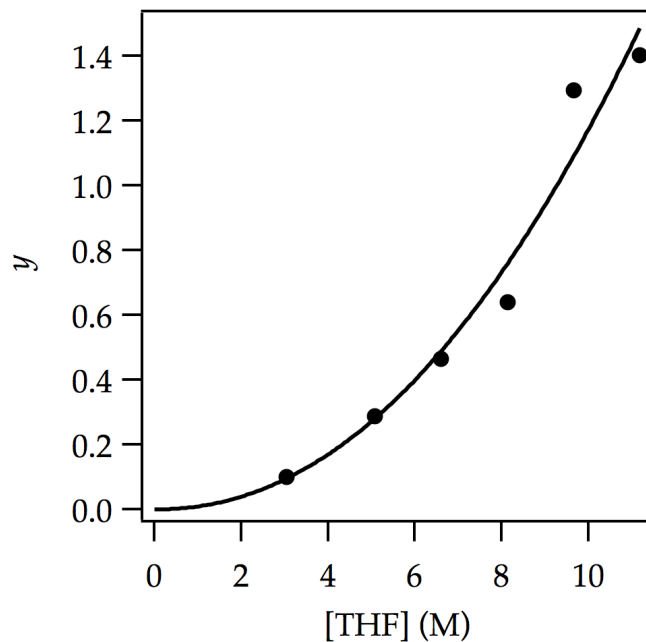


Figure 6. Plot of $\{[i\text{-Pr}_2\text{NH}][\text{ArLi}]\} / \{[\text{LDA}]^{(1/2)}[\text{ArH}]\}$ vs [THF] for the ortholithiation of **1** (0.005 M) with LDA (0.10 M) and diisopropylamine (0.025 M) at $-78\text{ }^\circ\text{C}$ measured by ^{19}F NMR spectroscopy. The curve depicts an unweighted least-squares fit to $y = K_{eq}[\text{THF}]^n$. [$K_{eq} = (9 \pm 7) \times 10^{-3}$, $n = (2.1 \pm 0.3)$]

[THF] (M)	y
11.18	1.40
9.66	1.29
8.13	0.64
6.61	0.46
5.08	0.29
3.05	0.10

Part 3: Rate Studies

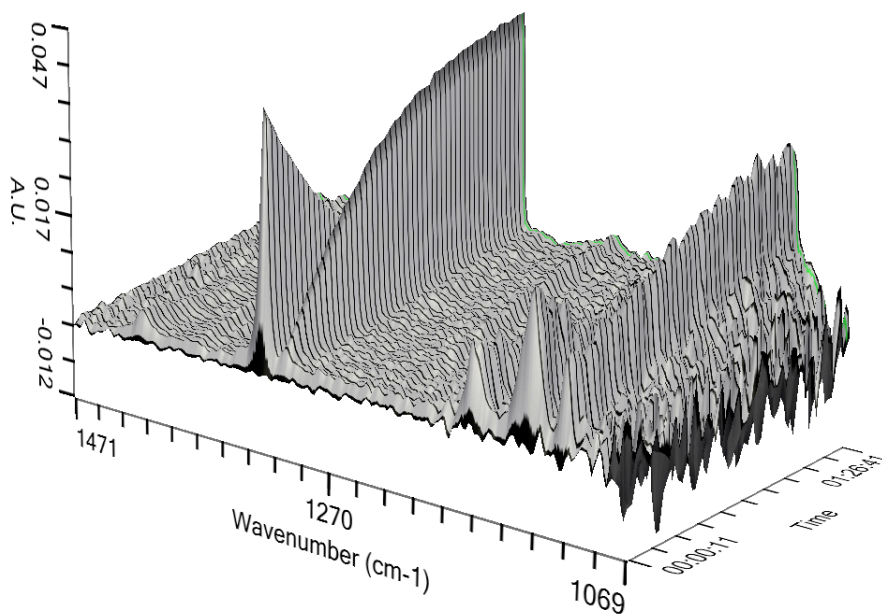


Figure 7. Representative in situ IR traces for the ortholithiation of **1** (0.005 M) by LDA (0.10 M) in THF at $-78\text{ }^{\circ}\text{C}$. IR absorptions for compounds **1** and **2** and their associated isotopomers are listed below. The IR spectra were deconvoluted using ConcIRT[®].

1: 1421 cm^{-1} , 1323 cm^{-1} , 1173 cm^{-1} , 1138 cm^{-1} , 1115 cm^{-1}
2: 1378 cm^{-1} , 1307 cm^{-1} , 1160 cm^{-1} , 1111 cm^{-1}

1- d_4 : 1448 cm^{-1} , 1348 cm^{-1} , 1253 cm^{-1} , 1156 cm^{-1} , 1136 cm^{-1} , 1026 cm^{-1}
2- d_3 : 1391 cm^{-1} , 1212 cm^{-1} , 1015 cm^{-1}

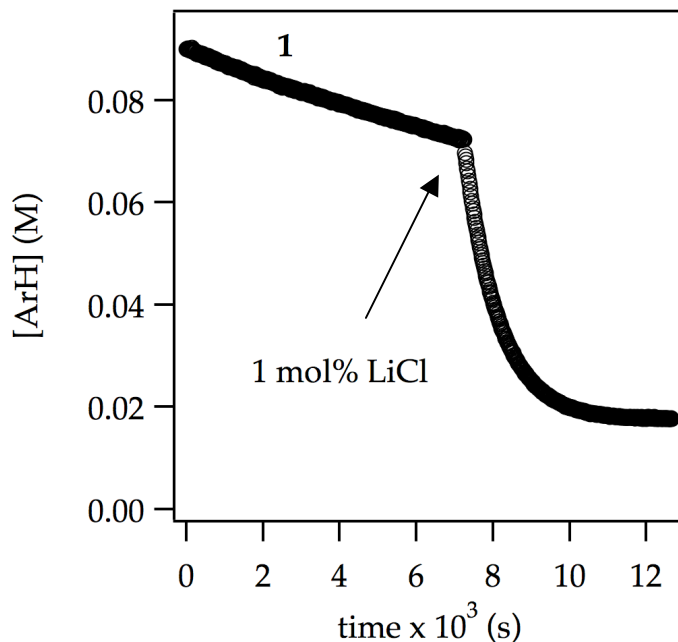


Figure 8. Ortholithiation of **1** (0.09 M) with LDA (0.10 M) in 12.2 M THF at $-78\text{ }^{\circ}\text{C}$ monitored by IR spectroscopy (1323 cm^{-1}) with injection of 1.0 mol % LiCl.

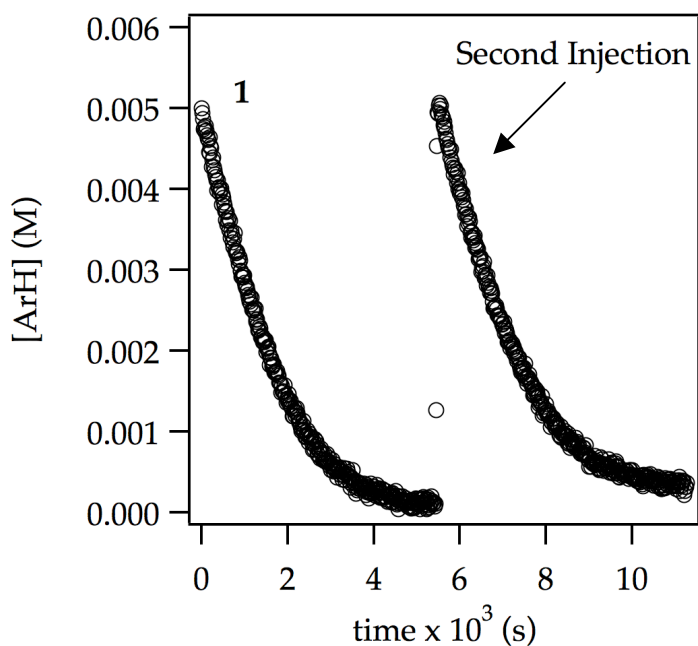


Figure 9. Representative plot showing concentration of arene **1** vs time for the ortholithiation of **1** (0.005 M) with LDA (0.10 M) in 12.2 M THF at $-78\text{ }^{\circ}\text{C}$. After the completion of the reaction, a second aliquot of **1** (0.005 M) was injected, showing no evidence of autocatalysis (catalysis by ArLi).

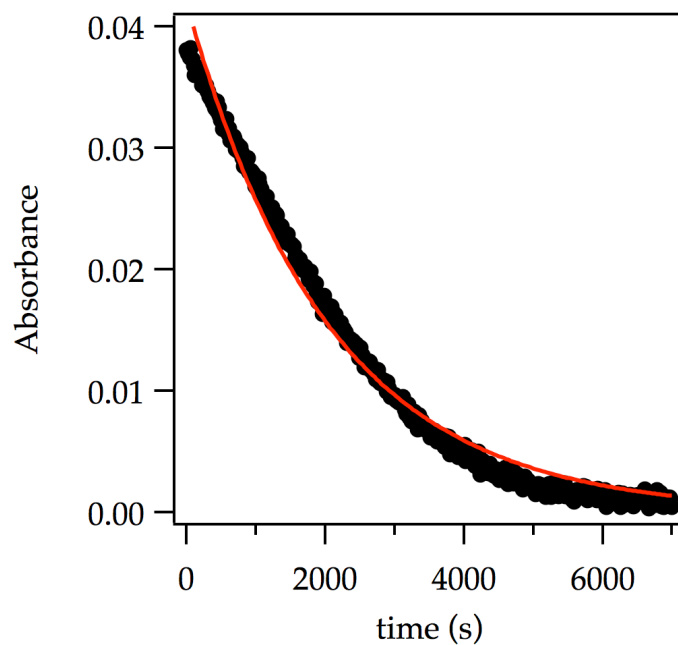


Figure 10. Representative plot showing poor exponential fit (red curve) to the decay of ortholithiation of **1** (0.005 M) with LDA (0.10 M) in THF (12.2 M) at -78 °C monitored by IR spectroscopy.

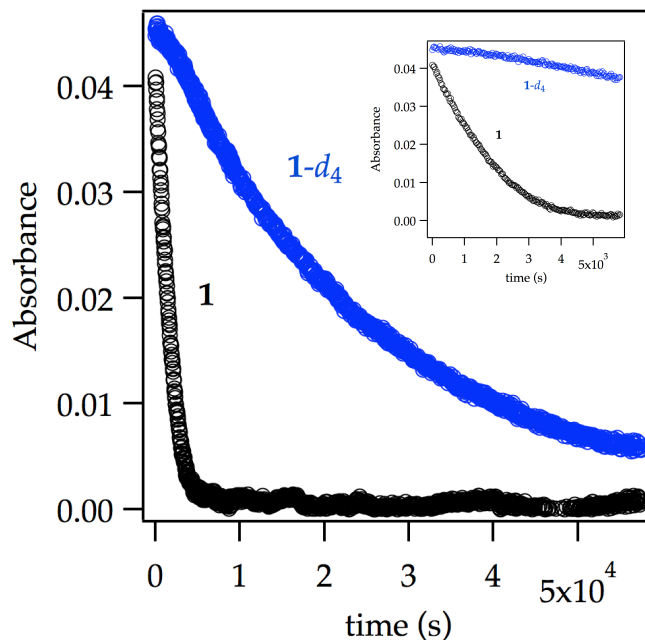


Figure 11. Competitive ortholithiation of **1** (0.005 M) and **1-d₄** (0.005 M) with LDA (0.10 M) in THF (12.2 M) at -78 °C. Monitoring absorbances of **1** and **1-d₄** at 1322 cm⁻¹ and 1253 cm⁻¹, respectively, by IR Spectroscopy affords $k_{\text{H}}/k_{\text{D}} = 21$.

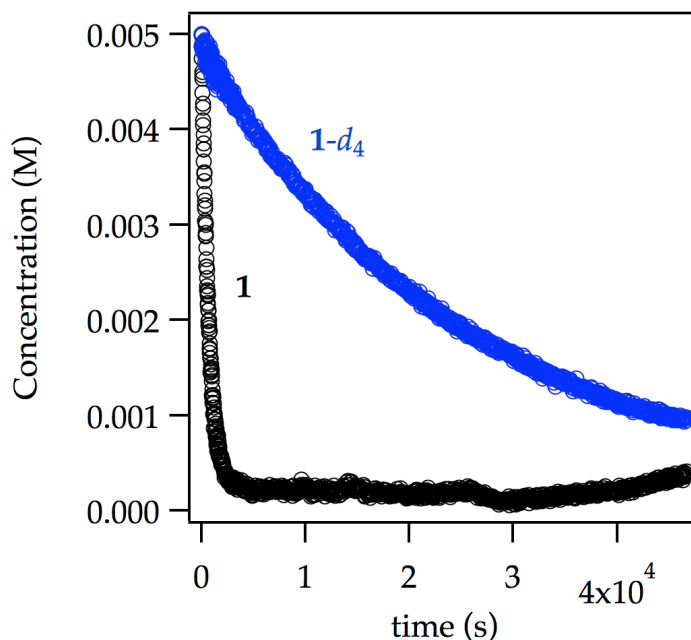


Figure 12. Competitive ortholithiation of **1** (0.005 M) and **1-d₄** (0.005 M) with LDA (0.10 M) in the presence of 1 mol % LiCl in THF (12.2 M) at -78 °C. Monitoring absorbances of **1** and **1-d₄** at 1322 cm⁻¹ and 1253 cm⁻¹, respectively, by IR Spectroscopy affords $k_{\text{H}}/k_{\text{D}} = 36$.

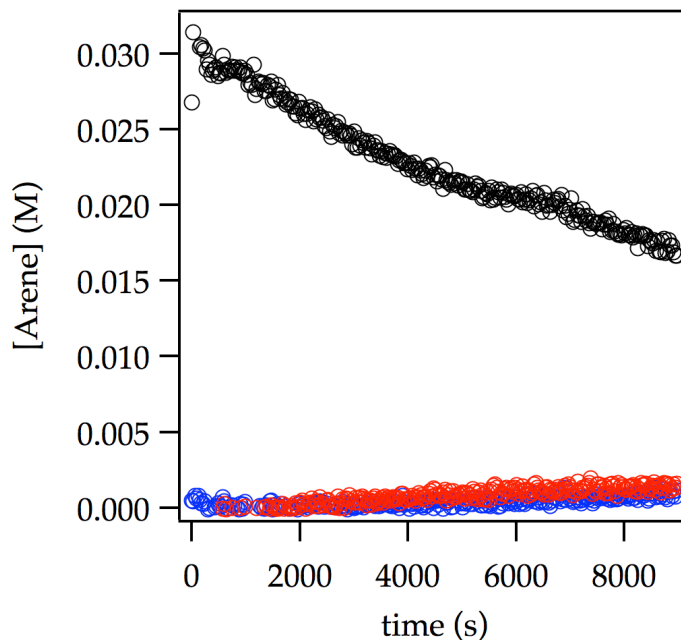
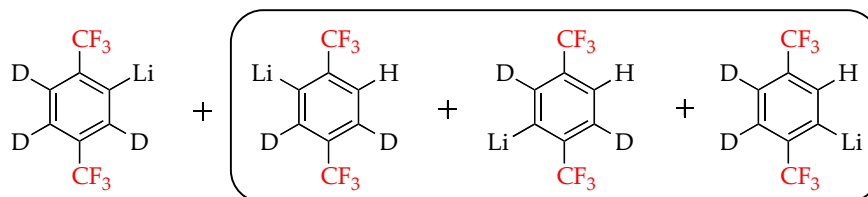


Figure 13. Ortholithiation of **1-*d*₃** (0.032 M) with LDA (0.10 M) in 12.2 M *d*₈-THF monitored by ¹H NMR. Percentages of regio-isomers were determined based on the initial rates of reactant decay (8.08 ppm) and products formation (7.11, 7.33, and 8.16 ppm). Theoretical percentages for the reversible and non-reversible mechanisms were derived from intramolecular (competitive) KIE.



Reversible	85%	5%	5%	5%
Non-reversible	47.5%	2.5%	25%	25%
Result	-----*	-----**	5.3%	6.5%

* Product not observed because no protons are present for detection

** Product not observed due to chemical shift overlap with benzene (*d*₈-THF impurity)

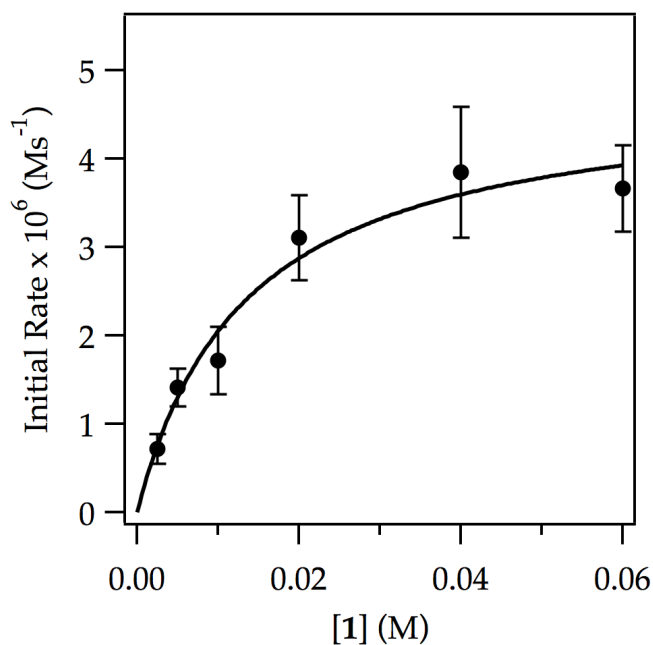


Figure 14. Plot of initial rate vs [ArH] (initial arene concentration) for the ortholithiation of **1** with LDA (0.050 M) in THF (12.2 M) at $-78\text{ }^{\circ}\text{C}$ as measured by IR spectroscopy. The curve depicts an unweighted least-squares fit to a first-order saturation function: $-\Delta[\text{ArH}]/\Delta t|_{t=0} = (a[\text{ArH}])/(1 + b[\text{ArH}])$. [$a = (3.6 \pm 0.7) \times 10^{-4}$, $b = (74 \pm 20)$]

[1] (M)	y_1 ($\text{M}\cdot\text{s}^{-1}$)	y_2 ($\text{M}\cdot\text{s}^{-1}$)
0.0025	8.37e-07	5.95e-07
0.005	1.56e-06	1.26e-06
0.01	1.45e-06	1.99e-06
0.02	2.77e-06	3.45e-06
0.04	3.32e-06	4.37e-06
0.06	4.01e-06	3.32e-06

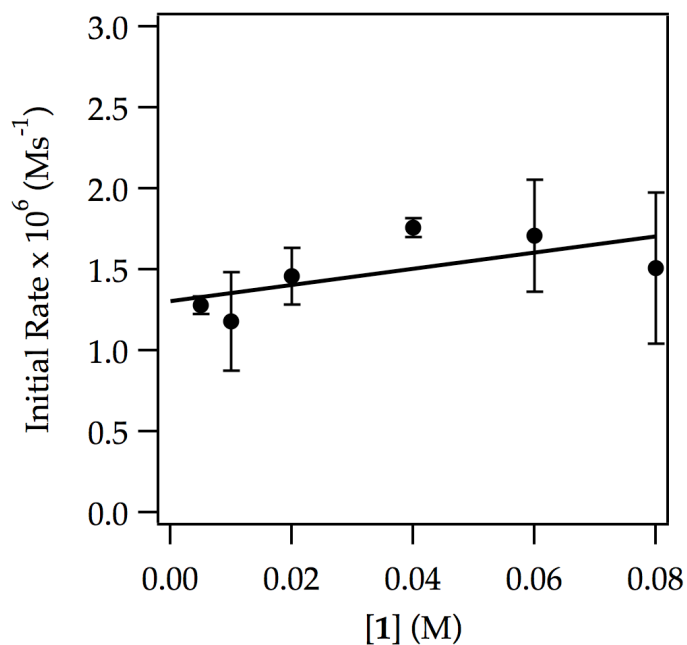


Figure 15. Plot of initial rate vs [ArH] (initial arene concentration) for the ortholithiation of **1** with LDA (0.20 M) in THF (3.05 M) at $-78\text{ }^{\circ}\text{C}$ as measured by IR spectroscopy. The curve depicts an unweighted least-squares fit to $y = a[\text{ArH}] + b$. [$a = (5 \pm 3) \times 10^{-6}$, $b = (1.3 \pm 0.1) \times 10^{-6}$]

[1] (M)	y_1 (Ms ⁻¹)	y_2 (Ms ⁻¹)	y_3 (Ms ⁻¹)
0.005	1.30e-06	1.33e-06	1.22e-06
0.01	1.40e-06	9.67e-07	-----
0.02	1.58e-06	1.33e-06	-----
0.04	1.80e-06	1.72e-06	-----
0.06	1.95e-06	1.46e-06	-----
0.08	1.18e-06	1.84e-06	-----

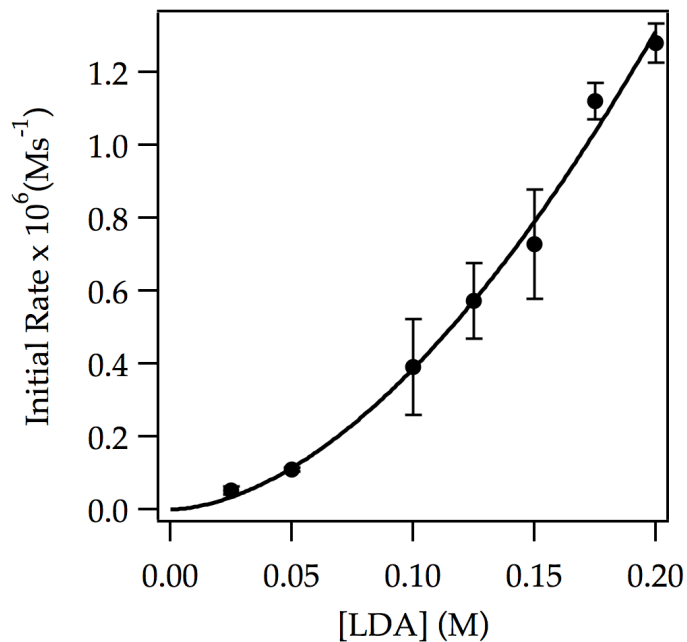


Figure 16. Plot of initial rate versus [LDA] in THF (3.05 M) for the ortholithiation of **1** (0.005 M) at $-78\text{ }^{\circ}\text{C}$ measured by IR spectroscopy. The curve depicts an unweighted least-squares fit to $y = a[\text{LDA}]^n$. [$a = (2.3 \pm 0.5) \times 10^{-5}$, $n = (1.8 \pm 0.1)$]

[LDA] (M)	y_1 (Ms ⁻¹)	y_2 (Ms ⁻¹)	y_3 (Ms ⁻¹)
0.025	5.99e-08	-----	4.31e-08
0.05	1.13e-07	-----	1.06e-07
0.10	3.04e-07	5.43e-07	3.27e-07
0.125	4.99e-07	-----	6.46e-07
0.150	5.60e-07	8.46e-07	7.76e-07
0.175	1.13e-06	1.17e-06	1.07e-06
0.20	1.30e-06	1.32e-06	1.22e-06

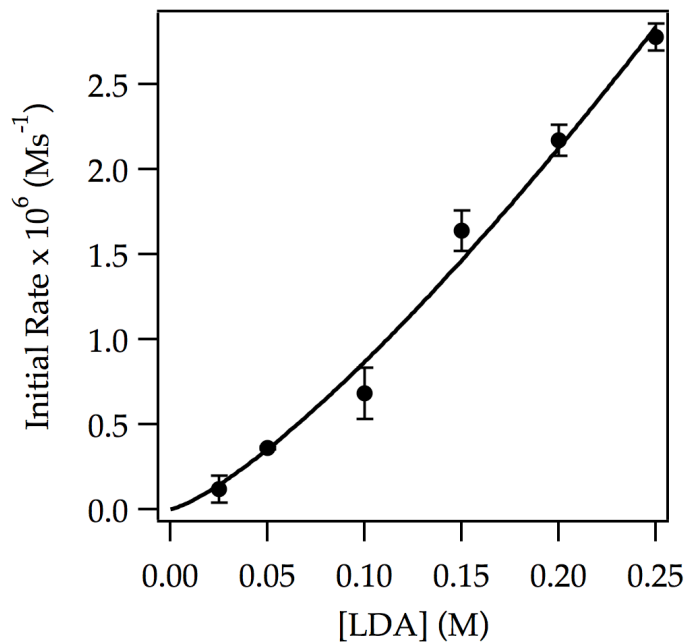


Figure 17. Plot of initial rate versus [LDA] in THF (6.10 M) for the ortholithiation of **1** (0.005 M) at $-78\text{ }^{\circ}\text{C}$ measured by IR spectroscopy. The curve depicts an unweighted least-squares fit to $y = a[\text{LDA}]^n$. [$a = (1.7 \pm 0.3) \times 10^{-5}$, $n = (1.3 \pm 0.1)$]

[LDA] (M)	y_1 ($\text{M}\cdot\text{s}^{-1}$)	y_2 ($\text{M}\cdot\text{s}^{-1}$)
0.025	1.76e-07	6.48e-08
0.05	3.53e-07	3.66e-07
0.10	7.87e-07	5.74e-07
0.15	1.72e-06	1.58e-06
0.20	2.23e-06	2.10e-06
0.25	2.83e-06	2.70e-06

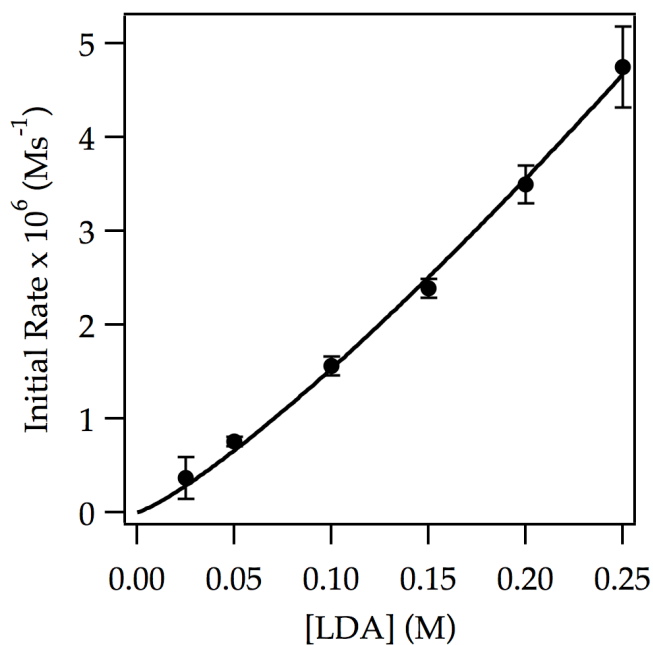


Figure 18. Plot of initial rate versus [LDA] in THF (9.15 M) for the ortholithiation of **1** (0.005 M) at $-78\text{ }^{\circ}\text{C}$ measured by IR spectroscopy. The curve depicts an unweighted least-squares fit to $y = a[\text{LDA}]^n$. [$a = (2.5 \pm 0.2) \times 10^{-5}$, $n = (1.22 \pm 0.05)$]

[LDA] (M)	y_1 (M·s ⁻¹)	y_2 (M·s ⁻¹)
0.025	5.27e-07	2.14e-07
0.05	7.17e-07	7.93e-07
0.10	1.64e-06	1.49e-06
0.15	2.47e-06	2.32e-06
0.20	3.65e-06	3.36e-06
0.25	5.06e-06	4.45e-06

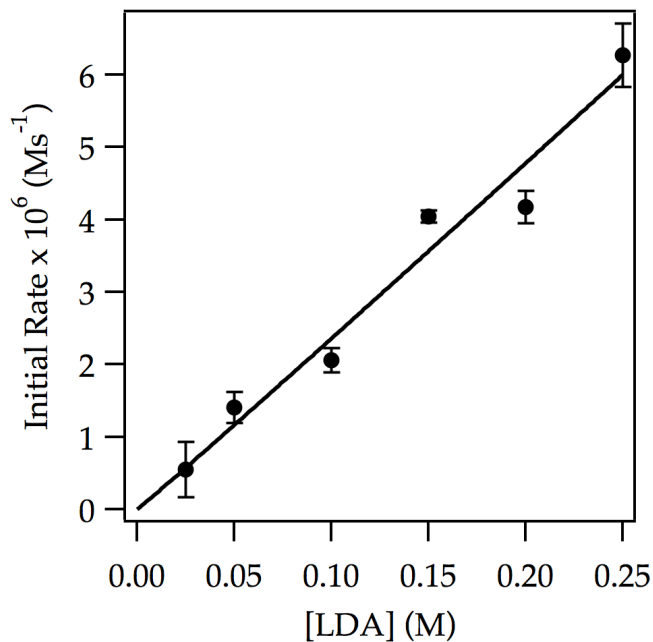


Figure 19. Plot of initial rate versus [LDA] in THF (12.2 M) for the ortholithiation of **1** (0.005 M) at $-78\text{ }^{\circ}\text{C}$ measured by IR spectroscopy. The curve depicts an unweighted least-squares fit to $y = a[\text{LDA}]^n$. [$a = (2.5 \pm 0.6) \times 10^{-5}$, $n = (1.0 \pm 0.1)$]

[LDA] (M)	y_1 (Ms ⁻¹)	y_2 (Ms ⁻¹)
0.025	8.16e-07	2.75e-07
0.05	1.56e-06	1.26e-06
0.10	2.18e-06	1.94e-06
0.15	3.98e-06	4.10e-06
0.20	4.02e-06	4.33e-06
0.25	6.58e-06	5.96e-06

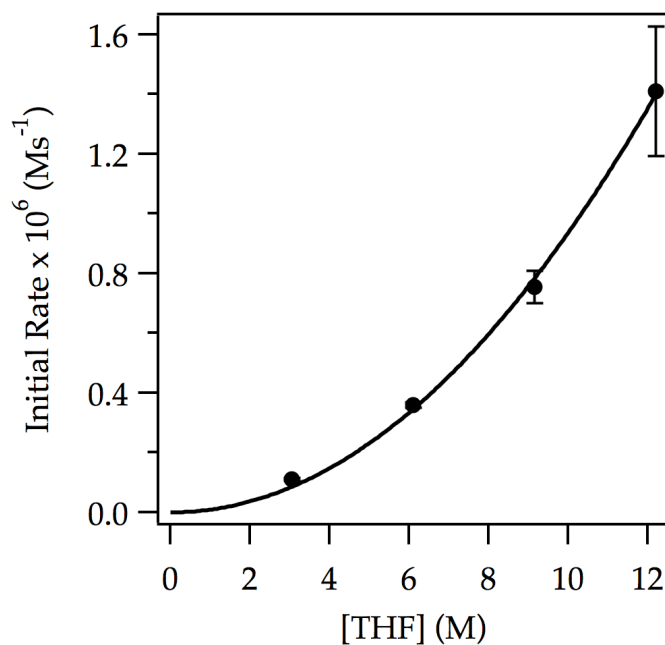


Figure 20. Plot of initial rate versus [THF] in hexanes for the ortholithiation of **1** (0.005 M) by LDA (0.050 M) at $-78\text{ }^{\circ}\text{C}$ measured by IR spectroscopy. The curve depicts an unweighted least-squares fit to $y = a[\text{THF}]^n$. [$a = (9 \pm 2) \times 10^{-9}$, $n = (2.0 \pm 0.1)$]

[THF] (M)	y_1 (Ms ⁻¹)	y_2 (Ms ⁻¹)
12.2	1.56e-06	1.26e-06
9.15	7.17e-07	7.93e-07
6.10	3.53e-07	3.66e-07
3.05	1.13e-07	1.06e-07

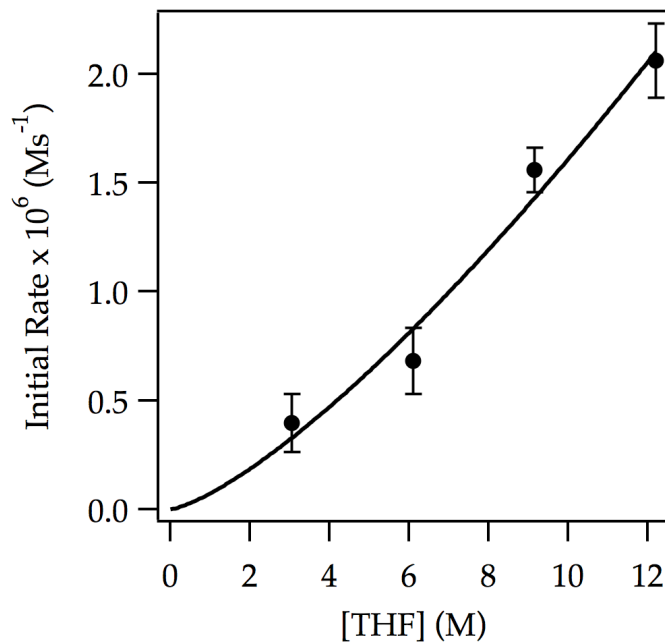


Figure 21. Plot of initial rate versus [THF] in hexanes for the ortholithiation of **1** (0.005 M) by LDA (0.10 M) at $-78\text{ }^{\circ}\text{C}$ measured by IR spectroscopy. The curve depicts an unweighted least-squares fit to $y = a[\text{THF}]^n$. [$a = (7 \pm 4) \times 10^{-8}$, $n = (1.3 \pm 0.2)$]

[THF] (M)	y_1 ($\text{M}\cdot\text{s}^{-1}$)	y_2 ($\text{M}\cdot\text{s}^{-1}$)	y_3 ($\text{M}\cdot\text{s}^{-1}$)
12.2	2.18e-06	1.94e-06	-----
9.15	1.64e-06	1.49e-06	-----
6.10	7.87e-07	5.74e-07	-----
3.05	3.04e-07	5.43e-07	3.27e-07

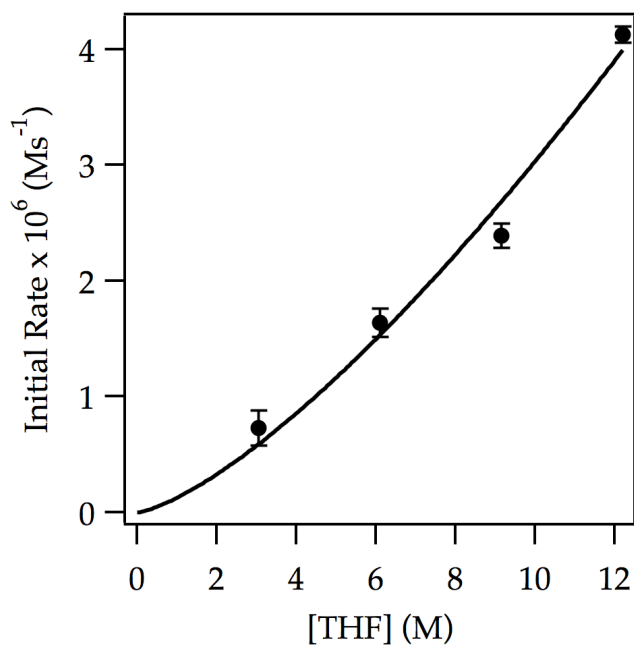


Figure 22. Plot of initial rate versus [THF] in hexanes for the ortholithiation of **1** (0.005 M) by LDA (0.15 M) at $-78\text{ }^{\circ}\text{C}$ measured by IR spectroscopy. The curve depicts an unweighted least-squares fit to $y = a[\text{THF}]^n$. [$a = (1.3 \pm 0.6) \times 10^{-7}$, $n = (1.4 \pm 0.2)$]

[THF] (M)	y_1 ($\text{M}\cdot\text{s}^{-1}$)	y_2 ($\text{M}\cdot\text{s}^{-1}$)	y_3 ($\text{M}\cdot\text{s}^{-1}$)
12.2	3.98e-06	4.10e-06	-----
9.15	2.47e-06	2.32e-06	-----
6.10	1.72e-06	1.55e-06	-----
3.05	5.60e-07	8.46e-07	7.76e-07

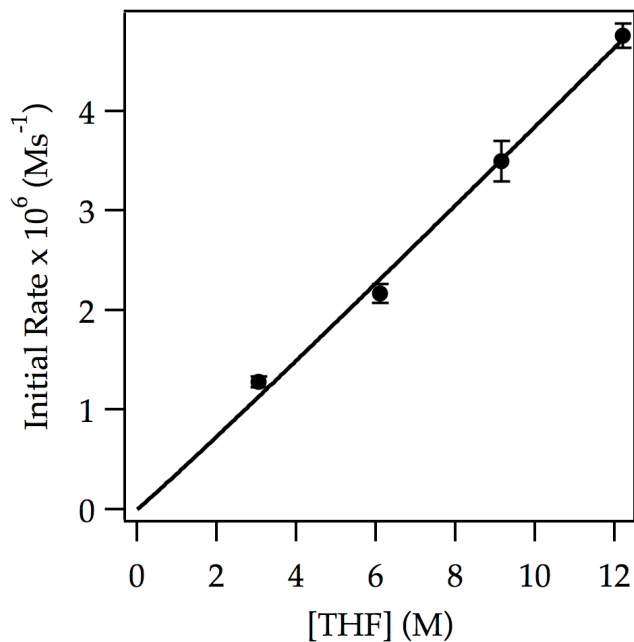


Figure 23. Plot of initial rate versus [THF] in hexanes for the ortholithiation of **1** (0.005 M) by LDA (0.20 M) at $-78\text{ }^{\circ}\text{C}$ measured by IR spectroscopy. The curve depicts an unweighted least-squares fit to $y = a[\text{THF}]^n$. [$a = (3.58 \pm 0.60) \times 10^{-7}$, $n = (1.03 \pm 0.07)$]

[THF] (M)	y_1 ($\text{M}\cdot\text{s}^{-1}$)	y_2 ($\text{M}\cdot\text{s}^{-1}$)	y_3 ($\text{M}\cdot\text{s}^{-1}$)
12.2	4.02e-06	4.33e-06	-----
9.15	3.65e-06	3.36e-06	-----
6.10	2.23e-06	2.10e-06	-----
3.05	1.30e-06	1.33e-06	1.22e-06

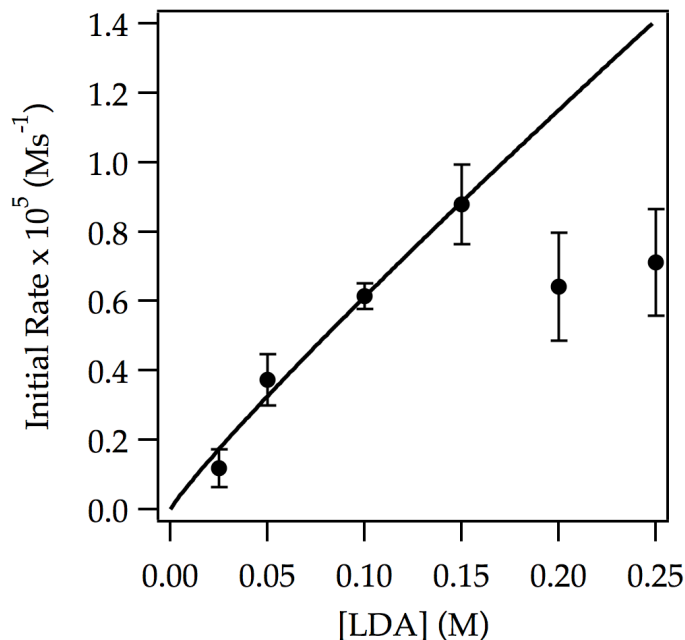


Figure 24. Plot of initial rate versus [LDA] in THF (12.2 M) for the ortholithiation of **1** (0.060 M) at $-78\text{ }^{\circ}\text{C}$ measured by IR spectroscopy. The curve depicts an unweighted least-squares fit to $y = a[\text{LDA}]^n$. [$a = (4 \pm 1) \times 10^{-5}$, $n = (0.9 \pm 0.1)$]
 *The deviation at 0.20 and 0.25 was recurring and not understood. It has the appearance of a phase change (precipitation), but we don't visually see evidence for this hypothesis nor have we observed it previously.

[LDA] (M)	y_1 ($\text{M}\cdot\text{s}^{-1}$)	y_2 ($\text{M}\cdot\text{s}^{-1}$)
0.025	8.00e-07	1.56e-06
0.05	3.32e-06	4.37e-06
0.10	6.40e-06	5.88e-06
0.15	9.59e-06	7.96e-06
0.20	7.50e-06	5.31e-06
0.25	8.21e-06	6.03e-06

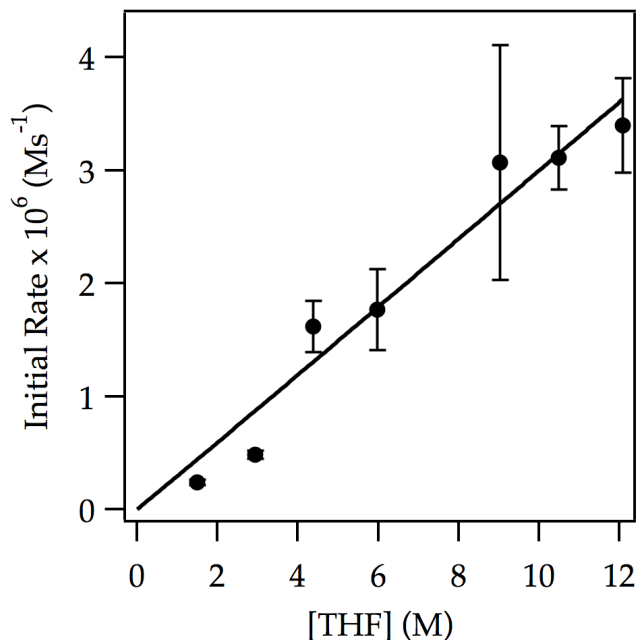


Figure 25. Plot of initial rate versus [THF] in hexanes for the ortholithiation of **1** (0.005 M) by LDA (0.20 M) at $-78\text{ }^{\circ}\text{C}$ measured by IR spectroscopy. The curve depicts an unweighted least-squares fit to $y = a[\text{THF}]^n$. [$a = (3 \pm 1) \times 10^{-7}$, $n = (1.0 \pm 0.1)$]

[THF] (M)	y_1 (M·s ⁻¹)	y_2 (M·s ⁻¹)	y_3 (M·s ⁻¹)	y_4 (M·s ⁻¹)
12.08	3.07e-06	3.21e-06	3.32e-06	4.01e-06
10.48	2.91e-06	3.31e-06	-----	-----
9.03	3.80e-06	2.33e-06	-----	-----
5.98	2.02e-06	1.51e-06	-----	-----
4.38	1.78e-06	1.46e-06	-----	-----
2.93	4.57e-07	5.05e-07	-----	-----
1.50	2.17e-07	2.54e-07	-----	-----

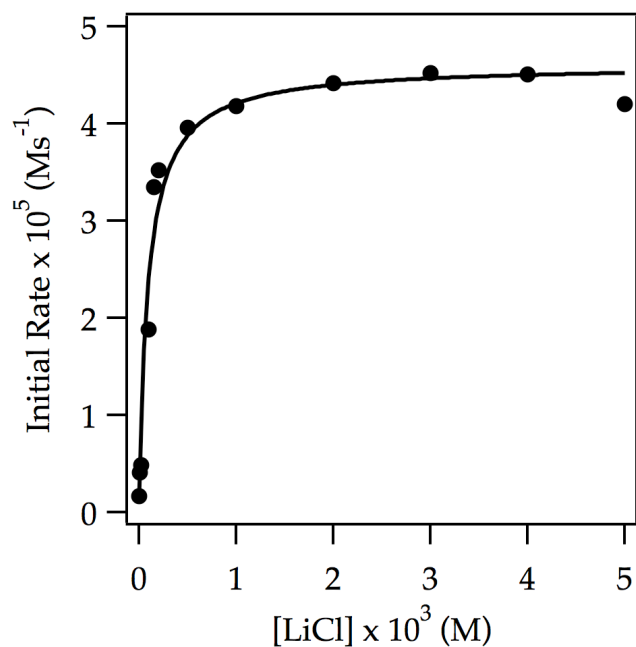


Figure 26. Plot of initial rate versus [LiCl] for the ortholithiation of **1** (0.05 M) by 0.10 M LDA in 12.2 M THF at $-78\text{ }^{\circ}\text{C}$ measured by IR spectroscopy. The curve depicts an unweighted least-squares fit to $-\Delta[\text{ArH}]/\Delta t|_{t=0} = (a[\text{LiCl}])/(1 + b[\text{LiCl}]) + c$. [$a = (4.5 \pm 0.8) \times 10^{-1}$, $b = (1.0 \pm 0.20) \times 10^4$, $c = (1.70) \times 10^{-6}$]

[LiCl x 10 ³] (M)	y_1 (Ms ⁻¹)
0.00	1.70e-07
0.01	4.08e-06
0.02	4.87e-06
0.10	1.88e-06
0.15	3.35e-06
0.20	3.52e-06
0.50	3.96e-06
1.00	4.18e-05
2.00	4.42e-05
3.00	4.52e-05
4.00	4.51e-05
5.00	4.20e-05

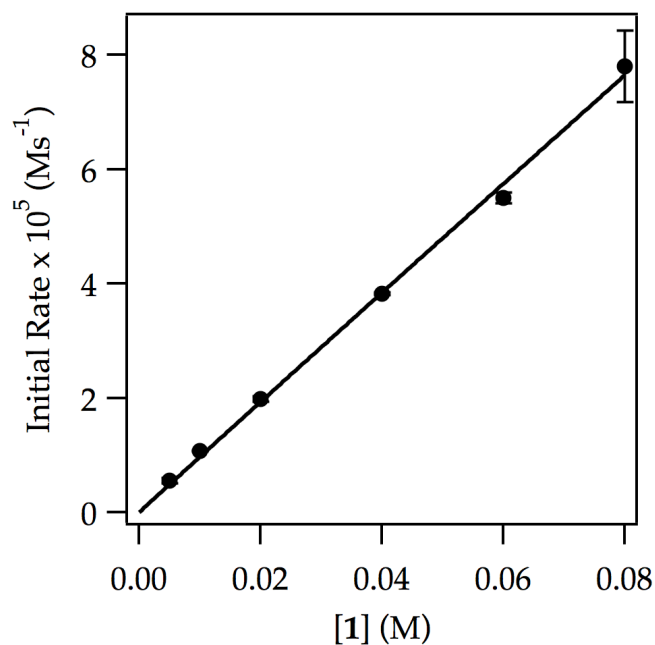


Figure 27. Plot of initial rate vs [ArH] (initial arene concentration) for the ortholithiation of **1** with LDA (0.10 M) in THF (12.2 M) with 1.0 mol% LiCl at -78 °C measured by IR spectroscopy. The curve depicts an unweighted least-squares fit to $y = a[\text{ArH}]^n$. [$a = (9 \pm 1) \times 10^{-4}$, $n = (0.99 \pm 0.04)$]

[1] (M)	y_1 (Ms ⁻¹)	y_2 (Ms ⁻¹)
0.005	5.19e-06	5.89e-06
0.01	1.06e-05	1.08e-05
0.02	2.02e-05	1.95e-05
0.04	3.85e-05	3.81e-05
0.06	5.57e-05	5.44e-05
0.08	8.25e-05	7.36e-05

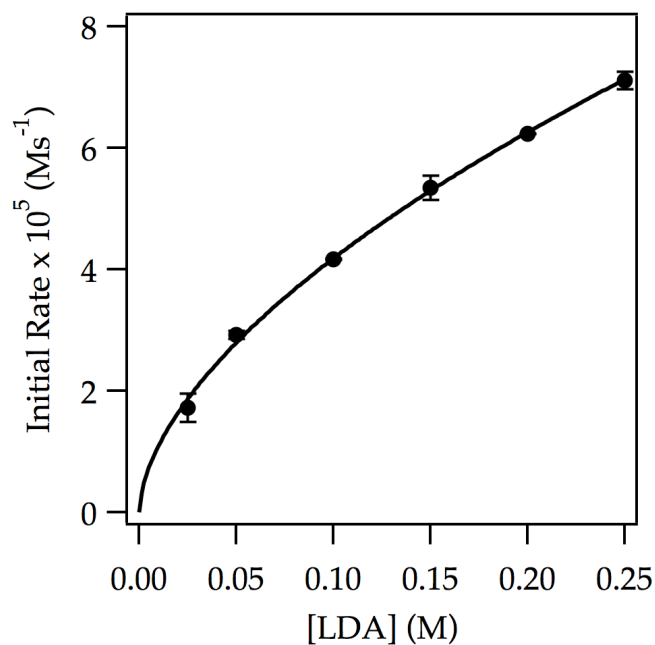


Figure 28. Plot of initial rate versus [LDA] in THF (12.2 M) for the ortholithiation of **1** (0.050 M) in the presence of 1.0 mol% LiCl at $-78\text{ }^{\circ}\text{C}$ measured by IR spectroscopy. The curve depicts an unweighted least-squares fit to $y = a[\text{LDA}]^n$. [$a = (1.60 \pm 0.05) \times 10^{-4}$, $n = 0.58 \pm 0.02$]

[LDA] (M)	y_1 ($\text{M}\cdot\text{s}^{-1}$)	y_2 ($\text{M}\cdot\text{s}^{-1}$)
0.025	1.88e-05	1.55e-05
0.05	2.96e-05	2.87e-05
0.10	4.17e-05	4.16e-05
0.15	5.49e-05	5.20e-05
0.20	6.23e-05	6.23e-05
0.25	7.00e-05	7.21e-05

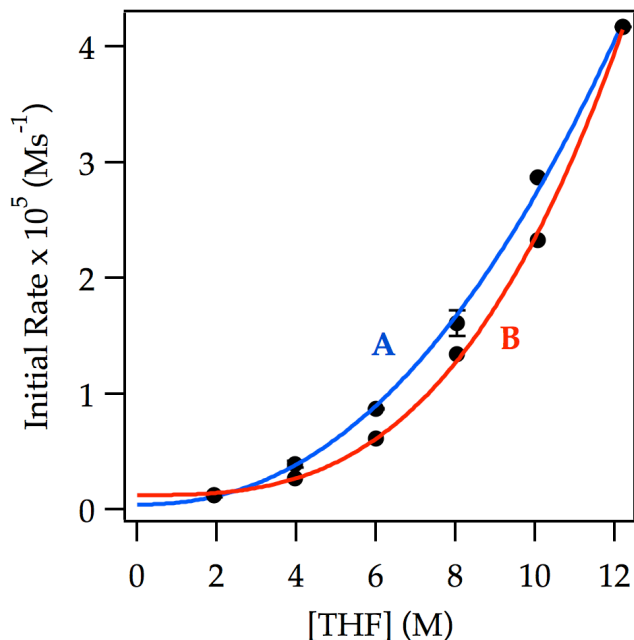


Figure 29. Plot of initial rate versus [THF] in Et₂O (curve A) and in hexanes (curve B) cosolvent for the ortholithiation of **1** (0.05 M) by LDA (0.10 M) in the presence of 1.0 mol% LiCl at -78 °C. The data was measured by IR spectroscopy. The curves depict unweighted least-squares fits to $y = a[\text{THF}]^n + b$. **Curve A:** $a = (1.8 \pm 0.3) \times 10^{-7}$, $n = 2.18 \pm 0.08$, $b = (0.0 \pm 0.1) \times 10^{-7}$. **Curve B:** $a = (2.3 \pm 0.7) \times 10^{-8}$, $n = 3.0 \pm 0.1$, $b = (1.2 \pm 0.4) \times 10^{-6}$.

[THF] (M)	$y_{1\text{-A}}$ (Ms ⁻¹)	$y_{2\text{-A}}$ (Ms ⁻¹)	$y_{3\text{-B}}$ (Ms ⁻¹)
12.2	4.17e-05	4.17e-05	4.17e-05
10.07	2.88e-05	2.86e-05	2.33e-05
8.03	1.53e-05	1.69e-05	1.34e-05
6.00	8.74e-06	8.64e-06	6.15e-06
3.97	3.71e-06	4.15e-06	2.66e-06
1.93	1.12e-06	1.38e-06	1.24e-06

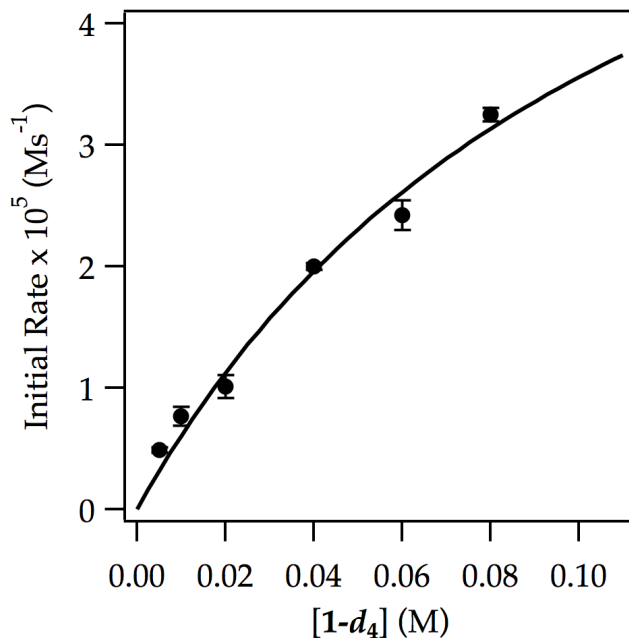


Figure 30. Plot of initial rate vs $[\text{ArD}_4]$ (initial arene concentration) for the ortholithiation of $\mathbf{1-d}_4$ with LDA (0.10 M) in THF (12.2 M) at -42°C measured by ^{19}F NMR spectroscopy. The curve depicts an unweighted least-squares fit to a first-order saturation function: $-\Delta[\text{ArD}_4]/\Delta t|_{t=0} = (a[\text{ArD}_4])/(1 + b[\text{ArD}_4])$. [$a = (6 \pm 1) \times 10^{-4}$, $b = (8 \pm 4)$]

$[\mathbf{1-d}_4]$ (M)	y_1 ($\text{M}\cdot\text{s}^{-1}$)	y_2 ($\text{M}\cdot\text{s}^{-1}$)
0.005	4.74e-06	5.09e-06
0.01	7.10e-06	8.20e-06
0.02	1.08e-05	9.47e-06
0.04	2.02e-05	1.98e-05
0.06	2.51e-05	2.34e-05
0.08	3.21e-05	3.29e-05

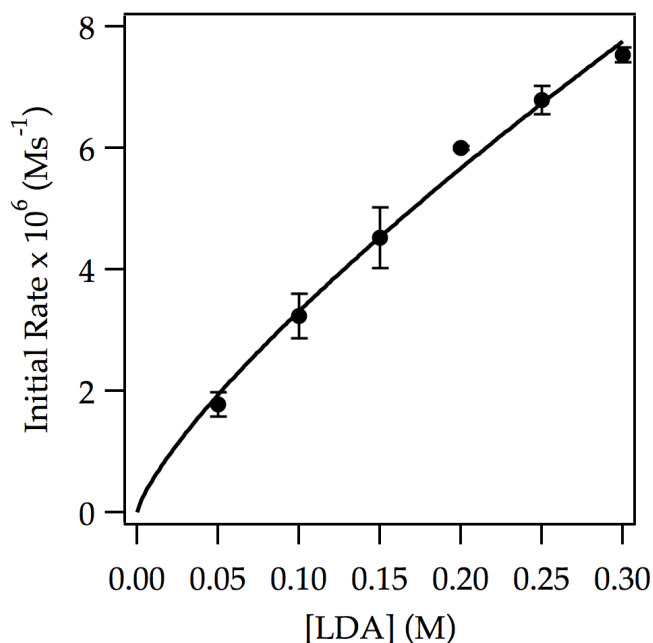


Figure 31. Plot of initial rate versus [LDA] in THF (12.2 M) for the ortholithiation of **1-d₄** (0.005 M) at $-42\text{ }^{\circ}\text{C}$ measured by ^{19}F NMR spectroscopy. The curve depicts an unweighted least-squares fit to $y = a[\text{LDA}]^n$. [$a = (2.0 \pm 0.1) \times 10^{-5}$, $n = 0.77 \pm 0.04$]

[LDA] (M)	y_1 (Ms ⁻¹)	y_2 (Ms ⁻¹)
0.05	1.64e-06	1.92e-06
0.10	2.98e-06	3.50e-06
0.15	4.18e-06	4.88e-06
0.20	5.98e-06	6.03e-06
0.25	6.63e-06	6.95e-06
0.30	7.45e-06	7.63e-06

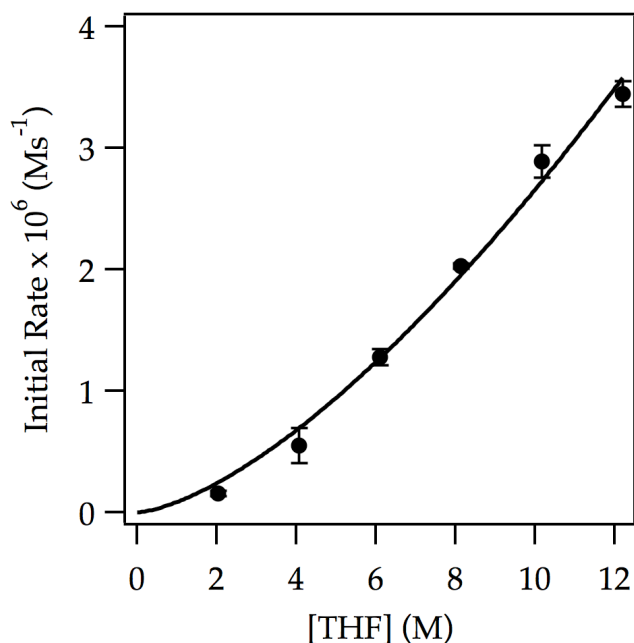


Figure 32. Plot of initial rate versus [THF] in Et₂O cosolvent for the ortholithiation of **1-d₄** (0.005 M) by LDA (0.10 M) at -42 °C measured by ¹⁹F NMR spectroscopy. The curve depicts an unweighted least-squares fit to $y = a[\text{THF}]^n$. [$a = (8 \pm 2) \times 10^{-5}$, $n = (1.5 \pm 0.1)$]

[THF] (M)	y_1 (M·s ⁻¹)	y_2 (M·s ⁻¹)
12.2	3.52e-06	3.37e-06
10.17	2.99e-06	2.80e-06
8.13	2.04e-06	2.03e-06
6.10	1.23e-06	1.33e-06
4.07	0.45e-06	0.66e-06
2.03	0.17e-06	0.14e-06

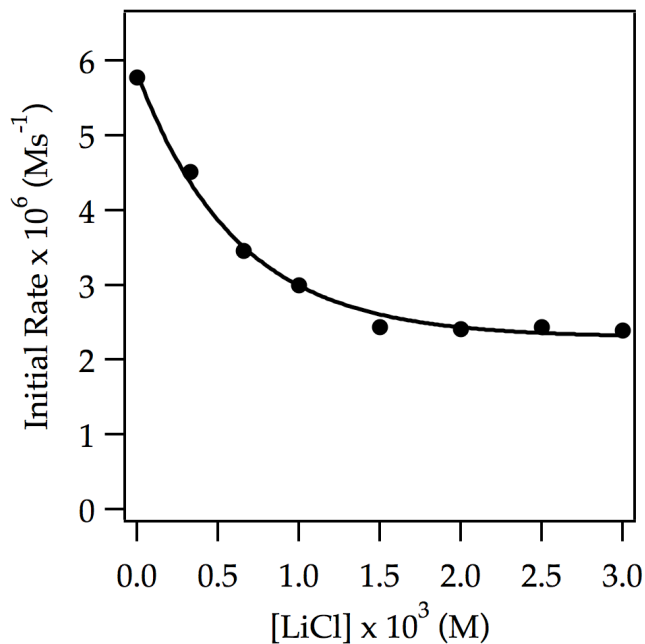


Figure 33. Plot of initial rate versus [LiCl] for the ortholithiation of **1-*d*₄** (0.005 M) by 0.30 M LDA in 12.2 M THF at $-42\text{ }^{\circ}\text{C}$ measured by ^{19}F NMR spectroscopy. The curve has no physical meaning.

[LiCl × 10 ³] (M)	y_1 (Ms ⁻¹)
0.00	5.78e-06
0.33	4.51e-06
0.66	3.46e-06
1.00	3.00e-06
1.50	2.44e-06
2.00	2.41e-06
2.50	2.44e-06
3.00	2.39e-06

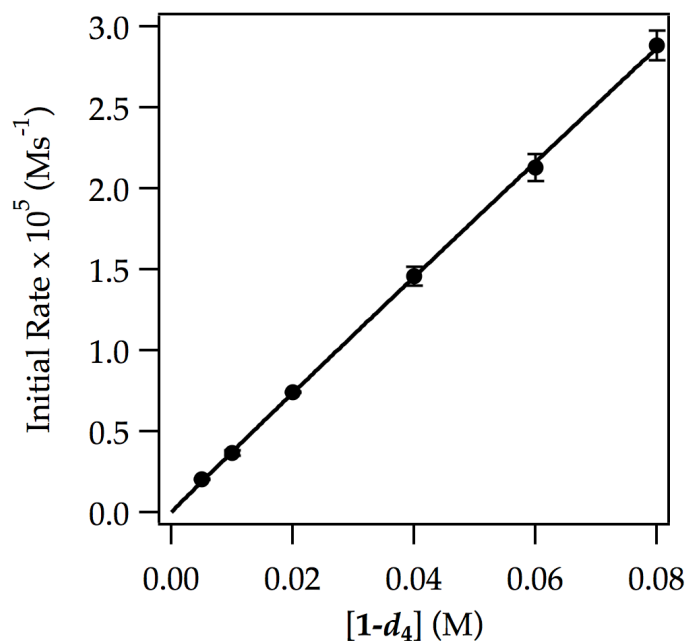


Figure 34. Plot of initial rate versus $[\text{ArD}_4]$ for the ortholithiation of $\mathbf{1-d}_4$ (0.005 M) by LDA (0.10 M) in the presence of 3.0 mol% LiCl at $-42\text{ }^\circ\text{C}$ measured by ^{19}F NMR spectroscopy. The curve depicts an unweighted least-squares fit to $y = a[\text{ArD}_4]^n$. [$a = (3.4 \pm 0.1) \times 10^{-4}$, $n = (0.98 \pm 0.01)$]

$[\mathbf{1-d}_4]$ (M)	y_1 (Ms ⁻¹)	y_2 (Ms ⁻¹)
0.005	2.03e-06	2.08e-06
0.01	3.79e-06	3.58e-06
0.02	7.46e-06	7.41e-06
0.04	1.50e-05	1.42e-05
0.06	2.19e-05	2.07e-05
0.08	2.82e-05	2.95e-05

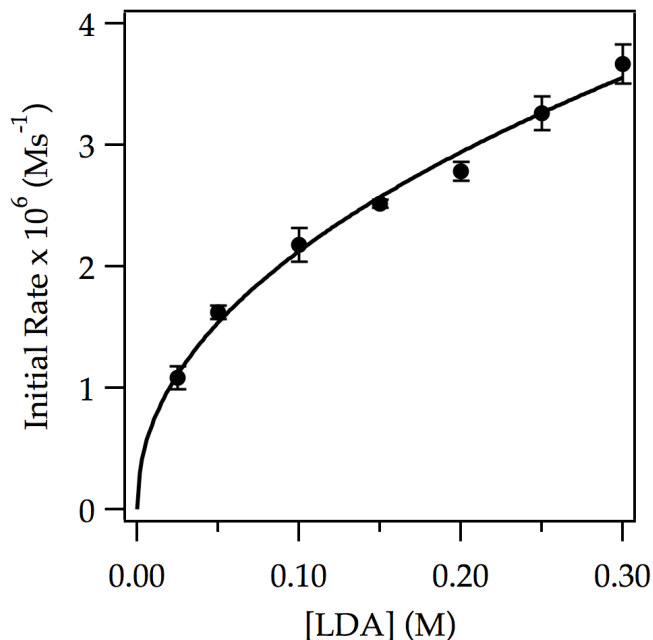


Figure 35. Plot of initial rate versus [LDA] in THF (12.2 M) for the ortholithiation of **1-d₄** (0.005 M) in the presence of 3.0 mol% LiCl at -42 °C measured by ¹⁹F NMR spectroscopy. The curve depicts an unweighted least-squares fit to $y = a[\text{LDA}]^n$. [$a = (6.2 \pm 0.3) \times 10^{-6}$, $n = 0.46 \pm 0.03$]

[LDA] (M)	y_1 (Ms ⁻¹)	y_2 (Ms ⁻¹)
0.025	1.02e-06	1.15e-06
0.05	1.58e-06	1.66e-06
0.10	2.08e-06	2.28e-06
0.15	2.54e-06	2.49e-06
0.20	2.73e-06	2.84e-06
0.25	3.16e-06	3.36e-06
0.30	3.55e-06	3.78e-06

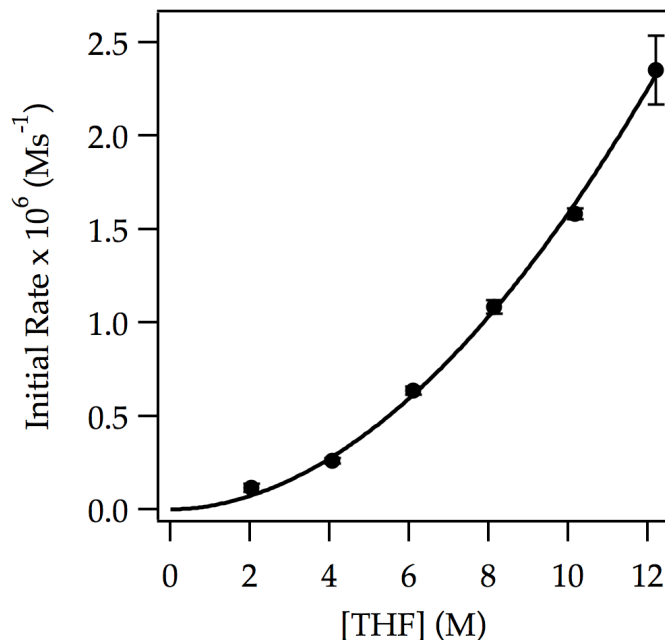


Figure 36. Plot of initial rate versus [THF] in Et₂O cosolvent for the ortholithiation of **1-d₄** (0.005 M) by LDA (0.10 M) in the presence of 3.0 mol% LiCl at -42 °C measured by ¹⁹F NMR spectroscopy. The curve depicts an unweighted least-squares fit to $y = a[\text{THF}]^n$. [$a = (1.9 \pm 0.3) \times 10^{-8}$, $n = (1.92 \pm 0.07)$]

[THF] (M)	y_1 (M·s ⁻¹)	y_2 (M·s ⁻¹)
12.2	2.48e-06	2.22e-06
10.17	1.56e-06	1.60e-06
8.13	1.06e-06	1.11e-06
6.10	6.20e-07	6.50e-07
4.07	2.50e-07	2.70e-07
2.03	1.30e-07	1.00e-07

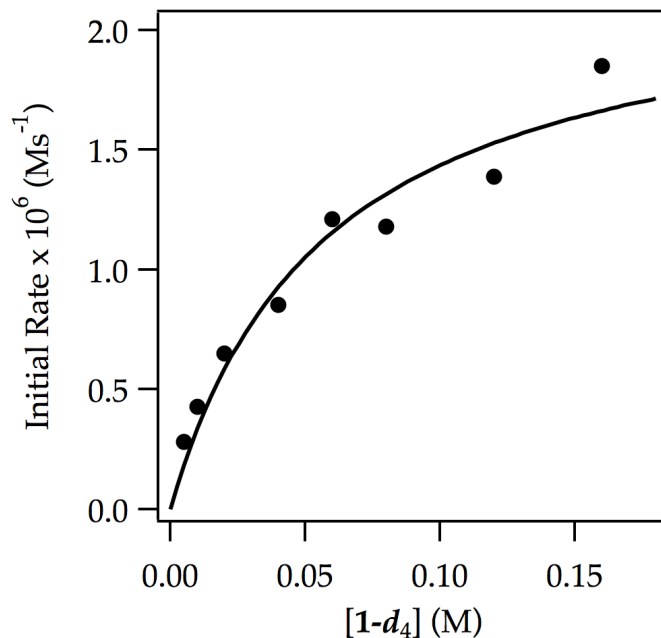


Figure 37. Plot of initial rate vs $[\text{ArD}_4]$ (initial arene concentration) for the ortholithiation of $\mathbf{1-d}_4$ with LDA (0.10 M) in THF (12.2 M) with at $-78\text{ }^\circ\text{C}$ measured by IR spectroscopy. The curve depicts an unweighted least-squares fit to a first-order saturation function: $-\Delta[\text{ArD}_4]/\Delta t|_{t=0} = (a[\text{ArD}_4])/(1 + b[\text{ArD}_4])$. [$a = (3.9 \pm 0.8) \times 10^{-5}$, $b = (17 \pm 5)$]

$[\mathbf{1-d}_4]$ (M)	y_1 (Ms ⁻¹)
0.005	2.81e-07
0.01	4.28e-07
0.02	6.51e-07
0.04	8.53e-07
0.06	1.21e-06
0.08	1.18e-06
0.12	1.39e-06
0.16	1.85e-06

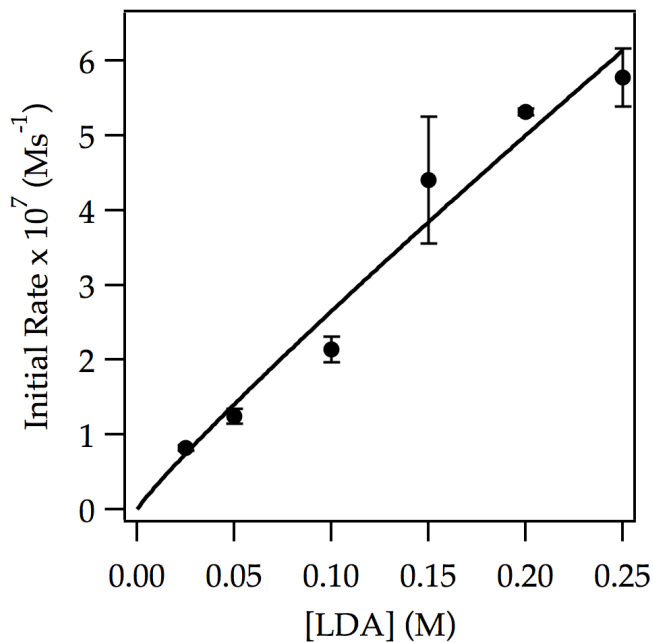


Figure 38. Plot of initial rate versus [LDA] in THF (12.2 M) for the ortholithiation of **1-d₄** (0.005 M) at -78 °C measured by IR spectroscopy. The curve depicts an unweighted least-squares fit to $y = a[\text{LDA}]^n$. [$a = (2.2 \pm 0.5) \times 10^{-6}$, $n = 0.9 \pm 0.1$]

[LDA] (M)	y_1 (Ms ⁻¹)	y_2 (Ms ⁻¹)
0.025	8.43e-06	7.98e-06
0.05	1.18e-06	1.32e-06
0.10	2.02e-06	2.26e-06
0.15	5.01e-06	3.81e-06
0.20	5.28e-06	5.35e-06
0.25	6.05e-06	5.50e-06

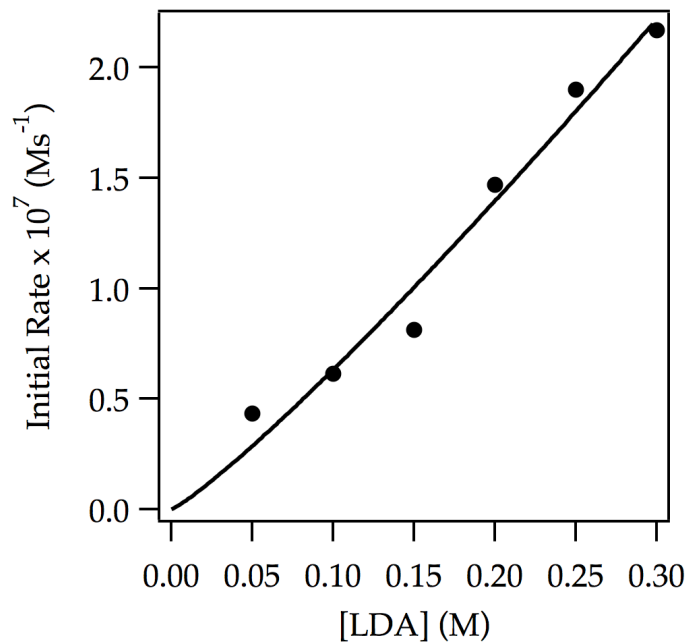


Figure 39. Plot of initial rate versus [LDA] in THF (3.05 M) for the ortholithiation of **1-d₄** (0.005 M) at -78 °C measured by IR spectroscopy. The curve depicts an unweighted least-squares fit to $y = a[\text{LDA}]^n$. [$a = (9 \pm 2) \times 10^{-7}$, $n = 1.1 \pm 0.1$]

[LDA] (M)	y_1 (Ms ⁻¹)
0.025	4.33e-08
0.05	6.13e-08
0.10	8.12e-08
0.15	1.47e-07
0.20	1.90e-07
0.25	2.17e-07

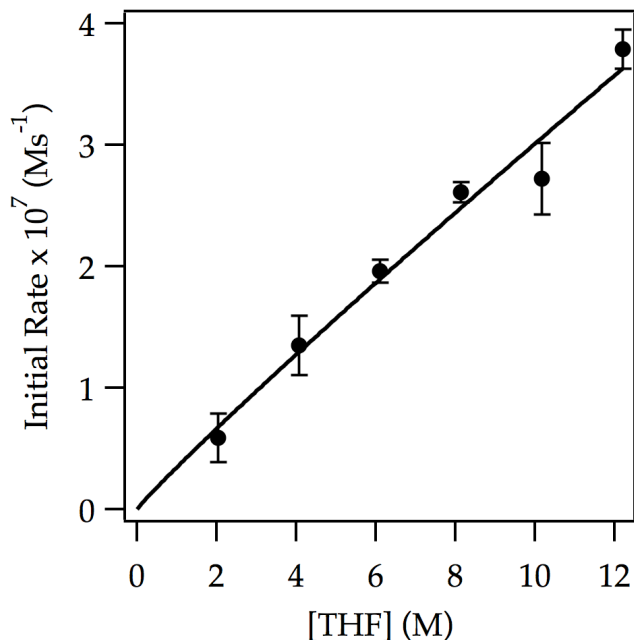


Figure 40. Plot of initial rate versus [THF] in hexanes for the ortholithiation of **1-*d*₄** (0.005 M) by LDA (0.10 M) at $-78\text{ }^{\circ}\text{C}$ measured by IR spectroscopy. The curve depicts an unweighted least-squares fit to $y = a[\text{THF}]^n$. [$a = (3.5 \pm 0.8) \times 10^{-8}$, $n = (0.94 \pm 0.09)$]

[THF] (M)	y_1 (M·s ⁻¹)	y_2 (M·s ⁻¹)
12.2	3.90e-07	3.67e-07
10.17	2.93e-07	2.51e-07
8.13	2.55e-07	2.67e-07
6.10	2.02e-07	1.89e-07
4.07	1.52e-07	1.17e-07
2.03	4.50e-08	7.31e-08

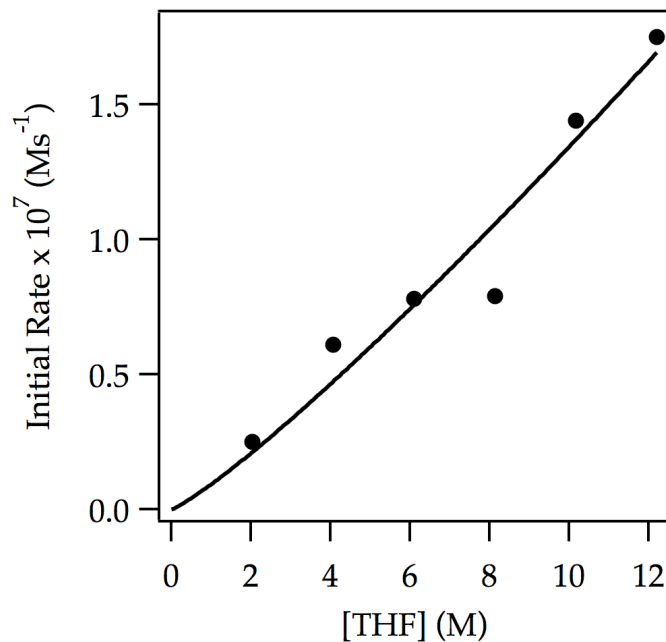


Figure 41. Plot of initial rate versus [THF] in hexanes for the ortholithiation of **1-*d*₄** (0.005 M) by LDA (0.050 M) at $-78\text{ }^{\circ}\text{C}$ measured by IR spectroscopy. The curve depicts an unweighted least-squares fit to $y = a[\text{THF}]^n$. [$a = (9 \pm 4) \times 10^{-9}$, $n = (1.2 \pm 0.2)$]

[THF] (M)	y_1 (Ms ⁻¹)
12.2	1.75e-07
10.17	1.44e-07
8.13	7.91e-08
6.10	7.79e-08
4.07	6.10e-08
2.03	2.51e-08

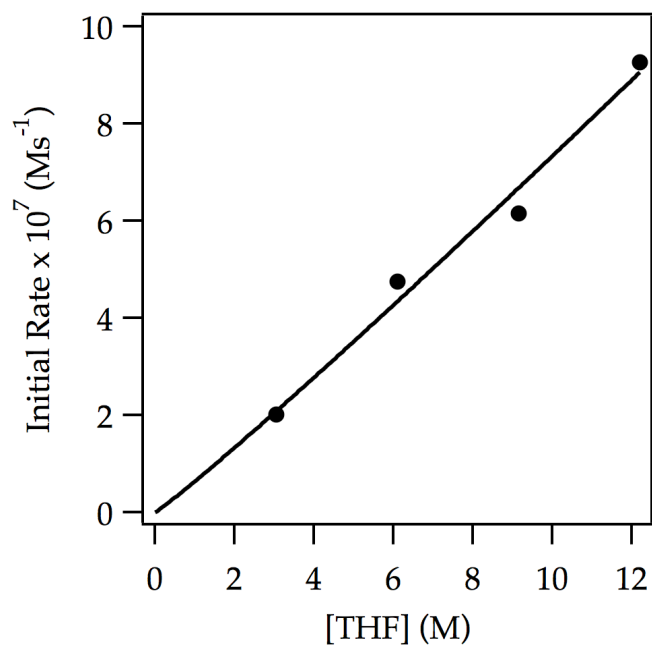


Figure 42. Plot of initial rate versus [THF] in hexanes for the ortholithiation of **1-*d*₄** (0.005 M) by LDA (0.20 M) at -78 °C measured by IR spectroscopy. The curve depicts an unweighted least-squares fit to $y = a[\text{THF}]^n$. [$a = (6 \pm 2) \times 10^{-8}$, $n = (1.1 \pm 0.1)$]

[THF] (M)	y_1 (Ms ⁻¹)
12.2	9.27e-07
9.15	6.15e-07
6.10	4.75e-07
3.05	2.01e-07

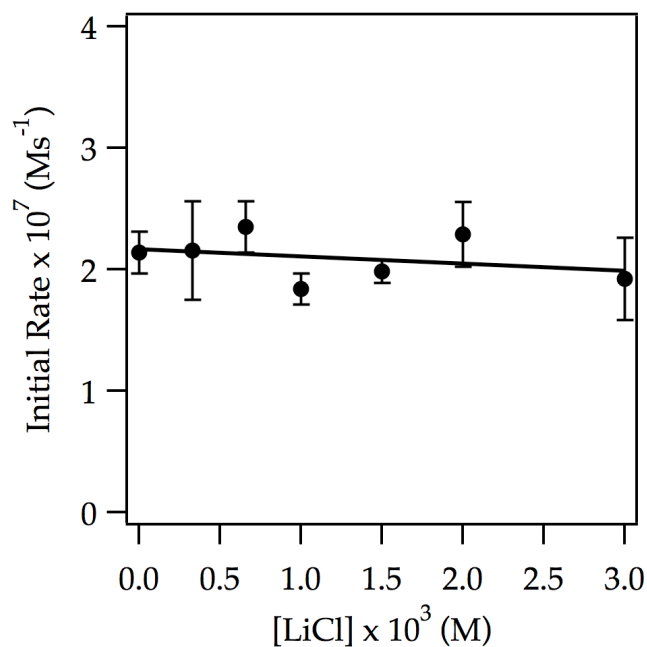


Figure 43. Plot of initial rate versus [LiCl] for the ortholithiation of **1-d₄** (0.005 M) by 0.10 M LDA in 12.2 M THF at -78 °C measured by IR spectroscopy. The curve depicts an unweighted least-squares fit to $y = a[\text{LiCl}] + b$. [$a = (6 \pm 8) \times 10^{-9}$, $b = (2.2 \pm 0.1) \times 10^{-7}$]

[LiCl] × 10 ³ (M)	y_1 (Ms ⁻¹)	y_2 (Ms ⁻¹)
0.00	2.02e-07	2.26e-07
0.33	2.44e-07	1.87e-07
0.66	2.20e-07	2.50e-07
1.00	1.93e-07	1.75e-07
1.50	2.05e-07	1.92e-07
2.00	2.48e-07	2.10e-07
3.00	2.16e-07	1.68e-07

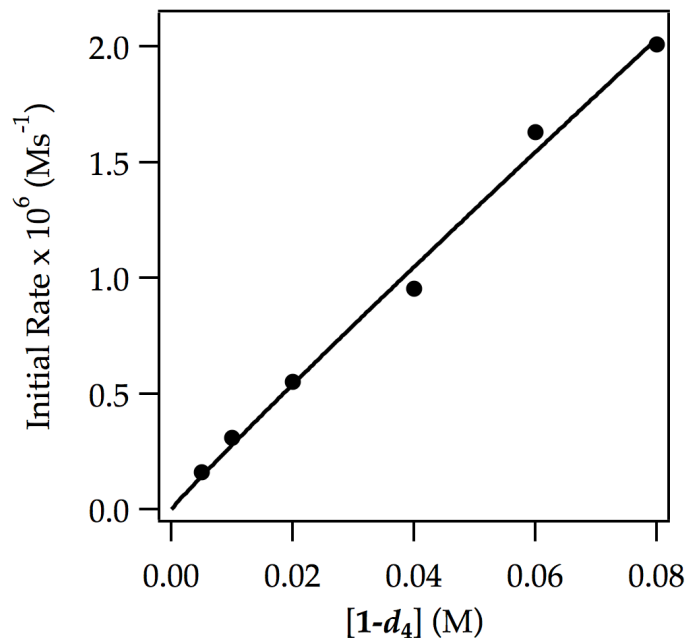


Figure 44. Plot of initial rate versus $[\text{ArD}_4]$ for the ortholithiation of $\mathbf{1-d}_4$ (0.005 M) by LDA (0.10 M) in the presence of 2.0 mol% LiCl at $-78\text{ }^\circ\text{C}$ measured by IR spectroscopy. The curve depicts an unweighted least-squares fit to $y = a[\text{ArD}_4]^n$. [$a = (2.3 \pm 0.4) \times 10^{-5}$, $n = (0.96 \pm 0.06)$]

$[\mathbf{1-d}_4]$ (M)	y_1 (Ms ⁻¹)
0.005	1.59e-07
0.01	3.08e-07
0.02	5.50e-07
0.04	9.53e-07
0.06	1.63e-06
0.08	2.01e-06

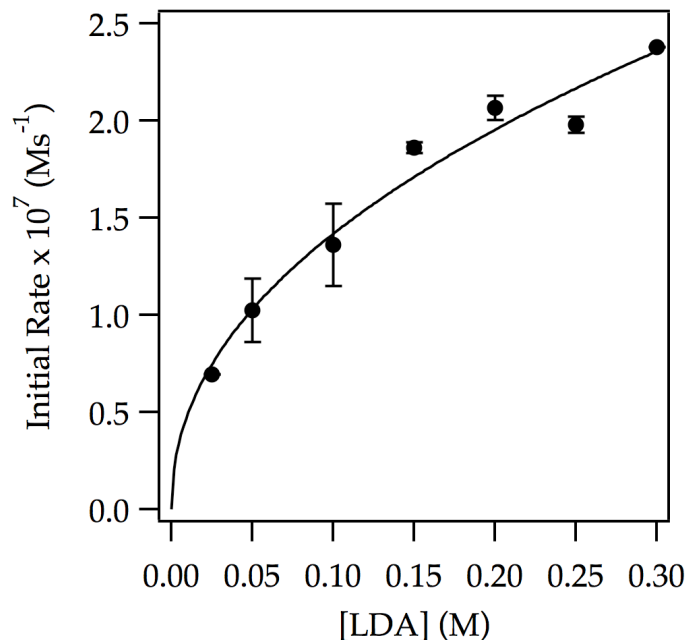


Figure 45. Plot of initial rate versus [LDA] in THF (12.2 M) for the ortholithiation of **1-d₄** (0.005 M) in the presence of 2.0 mol% LiCl at -78 °C measured by IR spectroscopy. The curve depicts an unweighted least-squares fit to $y = a[\text{LDA}]^n$. [$a = (4.1 \pm 0.4) \times 10^{-7}$, $n = 0.46 \pm 0.05$]

[LDA] (M)	y_1 (Ms ⁻¹)	y_2 (Ms ⁻¹)
0.025	6.96e-08	7.11e-06
0.05	9.08e-08	1.14e-07
0.10	1.51e-07	1.21e-07
0.15	1.84e-07	1.88e-07
0.20	2.02e-07	2.11e-07
0.25	2.01e-07	1.95e-07
0.30	2.38e-07	2.38e-07

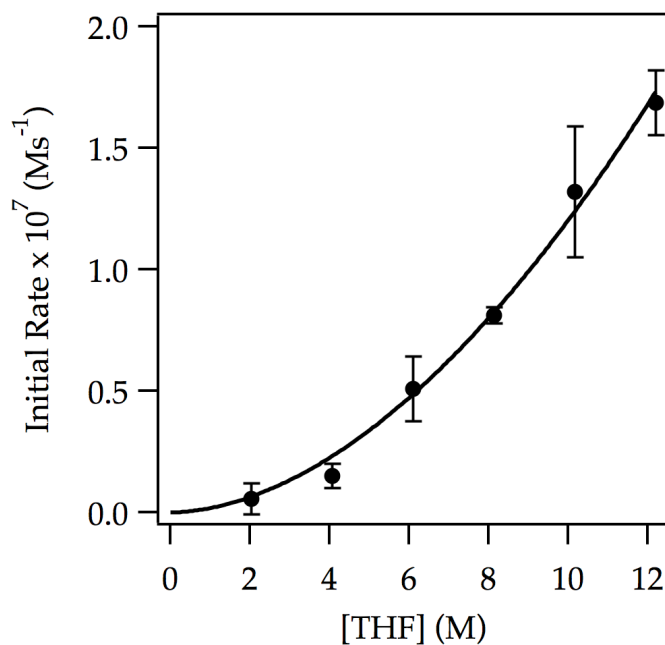


Figure 46. Plot of initial rate versus [THF] in Et₂O for the ortholithiation of **1-d₄** (0.005 M) by LDA (0.10 M) in the presence of 2.0 mol% LiCl at -78 °C measured by IR spectroscopy. The curve depicts an unweighted least-squares fit to $y = a[\text{THF}]^n$. [$a = (1.8 \pm 0.5) \times 10^{-9}$, $n = (1.8 \pm 0.1)$]

[THF] (M)	y_1 (M·s ⁻¹)	y_2 (M·s ⁻¹)
12.2	1.78e-07	1.59e-07
10.17	1.51e-07	1.13e-07
8.13	7.88e-08	8.36e-08
6.10	6.03e-08	4.16e-08
4.07	1.85e-08	1.16e-08
2.03	1.01e-08	9.20e-09

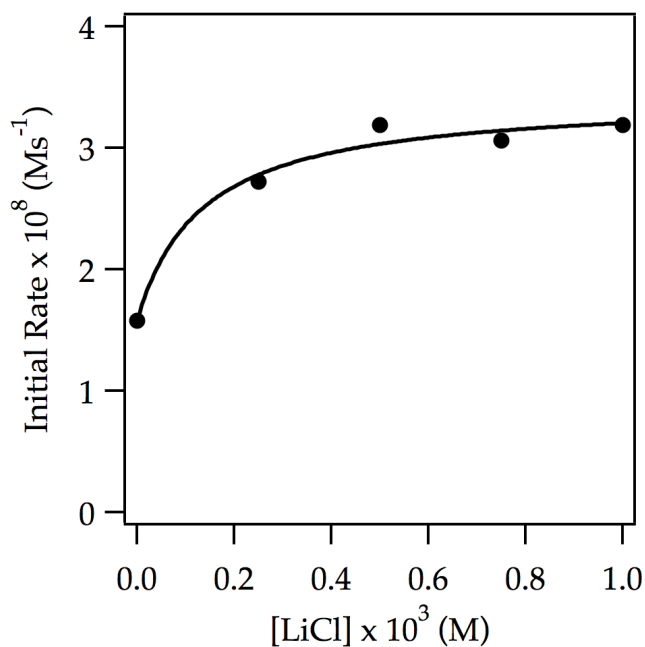


Figure 47. Plot of initial rate versus [LiCl] for the ortholithiation of **1-d₄** (0.005 M) by 0.10 M LDA in 12.2 M THF at -90 °C measured by IR spectroscopy. The curve depicts an unweighted least-squares fit to $-\Delta[\text{ArD}]/\Delta t|_{t=0} = (a[\text{LiCl}])/(1 + b[\text{LiCl}]) + c$. [$a = (1.4 \pm 0.5) \times 10^{-7}$, $b = 7 \pm 3$, $c = 1.58 \times 10^{-8}$]

[LiCl × 10 ³] (M)	y_1 (Ms ⁻¹)
0.00	1.58e-06
0.33	2.72e-06
0.66	3.19e-06
1.00	3.06e-06
1.50	3.19e-06

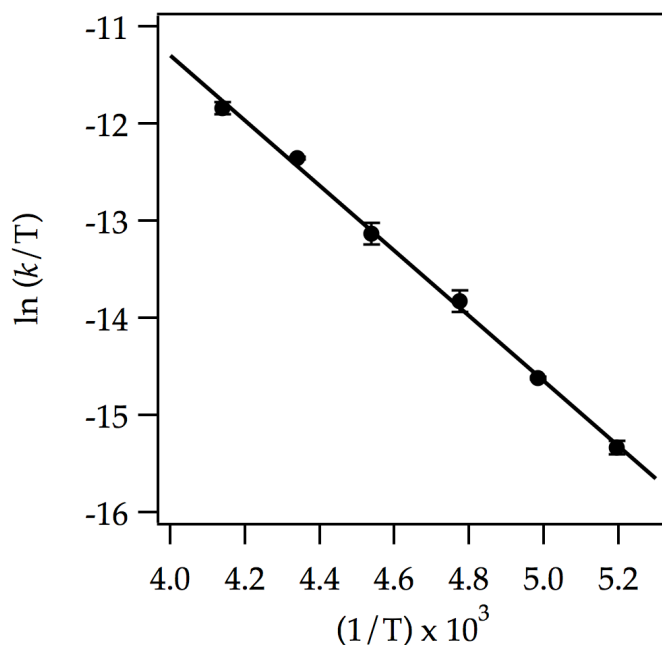
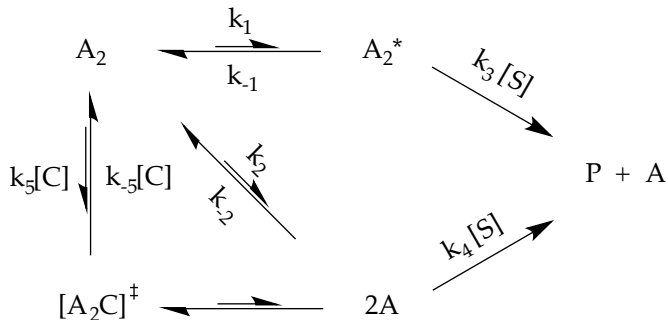


Figure 48. Plot of $\ln(k/T)$ versus $(1/T)$ for the ortholithiation of **1-d₄** (0.005 M) by LDA (0.10 M) in THF (12.2 M) at various temperatures measured by ¹⁹F NMR spectroscopy. The curve depicts an unweighted least-squares fit to $y = a(1/T) + b$. [$a = -(3.35 \pm 0.08) \times 10^3$, $b = (2.1 \pm 0.4)$]. Fit corresponds to $\Delta H^\ddagger = (6.6 \pm 0.2)$ kcal/mol and $\Delta S^\ddagger = (-43 \pm 8)$ cal/(molK).

Temperature (K)	$k_1(\text{M}^{-2}\text{s}^{-1})$	$k_2(\text{M}^{-2}\text{s}^{-1})$
241.55	1.82e-03	1.67e-03
230.45	1.01e-03	9.85e-03
220.35	4.03e-04	4.74e-04
209.45	2.14e-04	1.92e-04
200.65	8.92e-05	9.08e-05
192.45	4.44e-05	4.03e-05

Scheme 1. Scheme of dimer- and monomer-based lithations.



The system of differential equations that describes this mechanism follows.

$$\begin{aligned} \frac{d[A_2]}{dt} &= -k_1[A_2] + k_{-1}[A_2^*] - (k_2 + k_5[C])[A_2] + (k_{-2} + k_{-5}[C])[A]^2 \\ \frac{d[A_2^*]}{dt} &= k_1[A_2] - k_{-1}[A_2^*] - k_3[A_2^*][S] \\ \frac{d[A]}{dt} &= 2(k_2 + k_5[C])[A_2] - 2(k_{-2} + k_{-5}[C])[A]^2 - k_4[A][S] + k_3[A_2^*][S] \\ \frac{d[S]}{dt} &= -k_3[A_2^*][S] - k_4[A][S] \\ \frac{d[P]}{dt} &= k_3[A_2^*][S] + k_4[A][S] \end{aligned}$$

In order that the system conforms to mass balance both in the absence and presence of catalyst C, it must be that

$$k_{-5} = k_5 \frac{k_{-2}}{k_2}$$

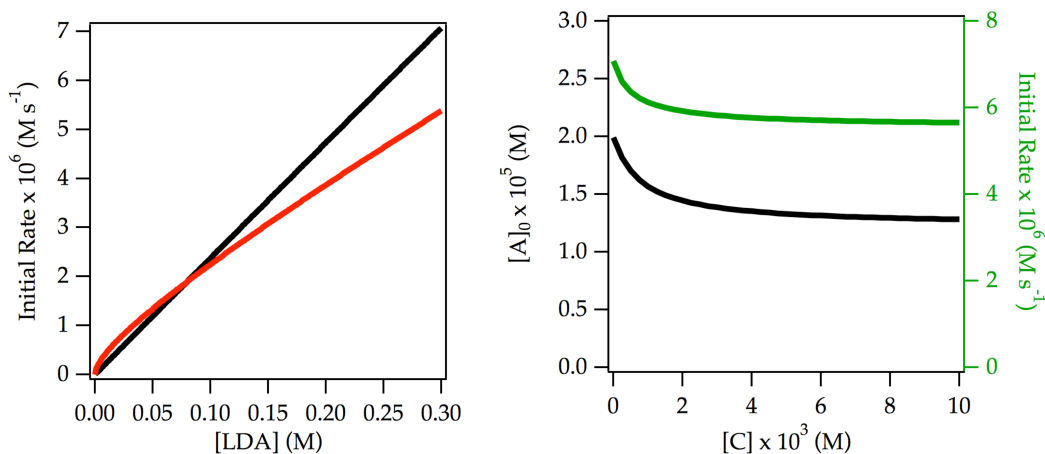


Figure 49. (a) Plot of initial rate vs [LDA]; (b) Plot of steady state $[A]_0$ and initial rate vs [C] at [LDA] = 0.30 M. The traces are produced by numerical integration of the differential equations described in Scheme 1 with $k_1 = 0.0005$, $k_{-1} = 0.5$, $k_2 = 1 \times 10^{-10}$, $k_{-2} = 0.1$, $k_3 = 5$, $k_4 = 30$, $k_5 = 0.005$, and $[S]_0 = 0.005 \text{ M}$. In plot (a), the black trace corresponds to $[C] = 0$, and the red trace corresponds to saturation in catalyst. Fitting the traces in plot (a) to $y = a[\text{LDA}]^n$ provides observed orders (black trace: $a = 2.34 \times 10^{-5}$, $n = 0.99$; red trace: $a = 1.37 \times 10^{-5}$, $n = 0.78$).

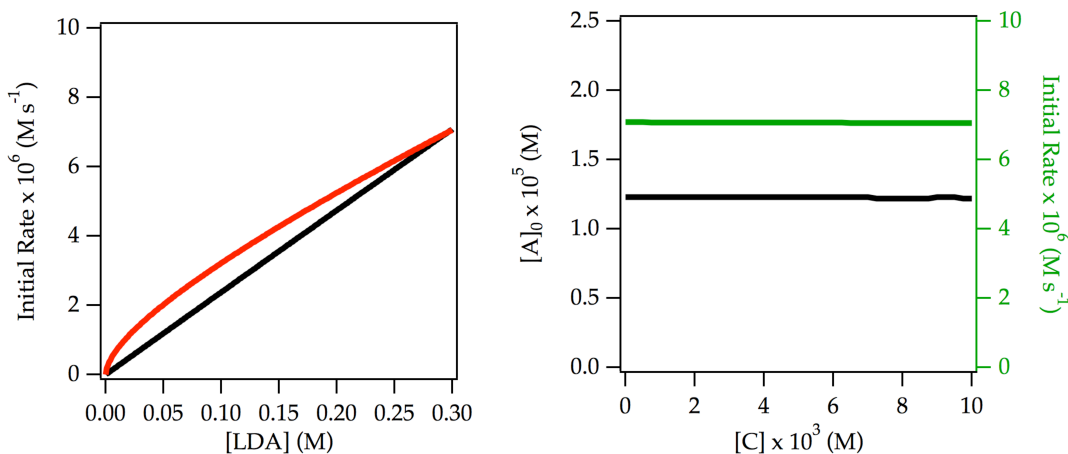


Figure 50. (a) Plot of initial rate vs [LDA]; (b) Plot of steady state $[A]_0$ and initial rate vs [C] at [LDA] = 0.30 M. The traces are produced by numerical integration of the differential equations described in Scheme 1 with $k_1 = 0.0005$, $k_{-1} = 0.5$, $k_2 = 1 \times 10^{-10}$, $k_{-2} = 0.1$, $k_3 = 5$, $k_4 = 58$, $k_5 = 0.005$, and $[S]_0 = 0.005 \text{ M}$. In plot (a), the black trace corresponds to $[C] = 0$, and the red trace corresponds to saturation in catalyst. Fitting the traces in plot (a) to $y = a[\text{LDA}]^n$ provides observed orders (black trace: $a = 2.35 \times 10^{-5}$, $n = 1.00$; red trace: $a = 1.63 \times 10^{-5}$, $n = 0.70$).

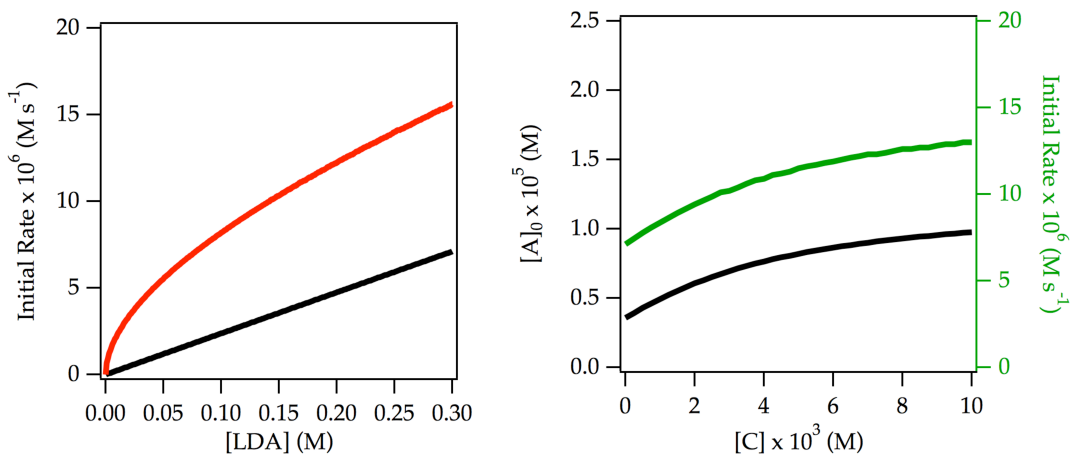


Figure 51. (a) Plot of initial rate vs [LDA]; (b) Plot of steady state $[A]_0$ and initial rate vs [C] at [LDA] = 0.30 M. The traces are produced by numerical integration of the differential equations described in Scheme 1 with $k_1 = 0.0005$, $k_{-1} = 0.5$, $k_2 = 1 \times 10^{-10}$, $k_{-2} = 0.1$, $k_3 = 5$, $k_4 = 200$, $k_5 = 0.005$, and $[S]_0 = 0.005 \text{ M}$. In plot (a), the black trace corresponds to $[C] = 0$, and the red trace corresponds to saturation in catalyst. Fitting the traces in plot (a) to $y = a[\text{LDA}]^n$ provides observed orders (black trace: $a = 2.36 \times 10^{-5}$, $n = 1.00$; red trace: $a = 3.11 \times 10^{-5}$, $n = 0.58$).

Part 4: Derivations

Derivation 1. Derivation of steady-state rate expressions:

Considering the mechanism depicted in Scheme 1, the rate of consumption of substrate is given by

$$-\frac{d[S]}{dt} = k_3[A_2^*][S] + k_4[A][S] \quad (1)$$

Use the mechanism to derive steady-state concentrations of A_2^* and A .

For open dimer A_2^* ,

$$\begin{aligned} \frac{d[A_2^*]}{dt} &= k_1[A_2] - k_{-1}[A_2^*] - k_3[A_2^*][S] = 0 \\ [A_2^*] &= \frac{k_1[A_2]}{k_{-1} + k_3[S]} \end{aligned} \quad (2)$$

For monomer A ,

$$\frac{d[A]}{dt} = 2(k_2 + k_5[C])[A_2] - 2(k_{-2} + k_5 \frac{k_{-2}}{k_2}[C])[A]^2 - k_4[A][S] + k_3[A_2^*][S] = 0 \quad (3)$$

Let $(k_2 + k_5[C]) = x$ and $(k_{-2} + k_5 \frac{k_{-2}}{k_2}[C]) = y$ so that

$$[A] = \frac{-k_4[S] + \sqrt{(k_4[S])^2 + 8y(2x[A_2] + k_3[A_2^*][S])}}{4y} \quad (4)$$

Insert equations (2) and (4) into (1) to give the rate of consumption of substrate as a function of the observables and microscopic rate constants:

$$-\frac{d[S]}{dt} = \frac{k_1 k_3 [A_2][S]}{k_{-1} + k_3[S]} + k_4 \left(\frac{-k_4[S] + \sqrt{(k_4[S])^2 + 8y \left(2x[A_2] + \frac{k_1 k_3 [A_2][S]}{k_{-1} + k_3[S]} \right)}}{4y} \right) [S] \quad (5)$$

Analysis of limiting cases:

No catalyst:

In the absence of catalyst, $x = k_2$ and $y = k_{-2}$, so equation (5) becomes

$$-\frac{d[S]}{dt} = \frac{k_1 k_3 [A_2][S]}{k_{-1} + k_3 [S]} + k_4 \left(\frac{-k_4 [S] + \sqrt{(k_4 [S])^2 + 8k_{-2} \left(2k_2 [A_2] + \frac{k_1 k_3 [A_2][S]}{k_{-1} + k_3 [S]} \right)}}{4k_{-2}} \right) [S]$$

Assume that the basal deaggregation to monomer is negligible relative to the contribution from dimer metalation, i.e. $2k_2 [A_2] \ll \frac{k_1 k_3 [A_2][S]}{k_{-1} + k_3 [S]}$, so that

$$-\frac{d[S]}{dt} = \frac{k_1 k_3 [A_2][S]}{k_{-1} + k_3 [S]} + k_4 \left(\frac{-k_4 [S] + \sqrt{(k_4 [S])^2 + 8k_{-2} \frac{k_1 k_3 [A_2][S]}{k_{-1} + k_3 [S]}}}{4k_{-2}} \right) [S] \quad (6)$$

An altogether different route to a similar end is to assume that the contribution of basal deaggregation to the monomer is negligible in equation (3) by way

of $2(k_2 + k_5 [C])[A_2] - 2(k_{-2} + k_5 \frac{k_{-2}}{k_2} [C])[A]^2 \ll -k_4 [A][S] + k_3 [A_2^*][S]$, so that equation (3) becomes

$$[A] = \frac{k_3}{k_4} [A_2^*]$$

and therefore the rate law for consumption of substrate, equation (1), becomes

$$-\frac{d[S]}{dt} = 2 \frac{k_1 k_3 [A_2][S]}{k_{-1} + k_3 [S]} \quad (7)$$

Full catalyst saturation:

With $[C] \gg 0$, $x \approx k_5[C]$ and $y \approx k_5 \frac{k_{-2}}{k_2}[C]$, so equation (5) becomes

$$-\frac{d[S]}{dt} = \frac{k_1 k_3 [A_2][S]}{k_{-1} + k_3 [S]} + k_4 \left(\frac{-k_4 [S] + \sqrt{(k_4 [S])^2 + 8k_5 \frac{k_{-2}}{k_2} [C] \left(2k_5 [C][A_2] + \frac{k_1 k_3 [A_2][S]}{k_{-1} + k_3 [S]} \right)}}{4k_5 \frac{k_{-2}}{k_2} [C]} \right) [S]$$

Noting that $2k_5 [C][A_2] \gg \frac{k_1 k_3 [A_2][S]}{k_{-1} + k_3 [S]}$ gives

$$-\frac{d[S]}{dt} = \frac{k_1 k_3 [A_2][S]}{k_{-1} + k_3 [S]} + k_4 \left(\frac{-k_4 [S] + \sqrt{(k_4 [S])^2 + 16(k_5 [C])^2 \frac{k_{-2}}{k_2} [A_2]}}{4k_5 \frac{k_{-2}}{k_2} [C]} \right) [S]$$

Given that the second term under the radical can grow indefinitely, i.e.

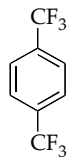
$(k_4 [S])^2 \ll 16(k_5 [C])^2 \frac{k_{-2}}{k_2} [A_2]$, one has

$$-\frac{d[S]}{dt} = \frac{k_1 k_3 [A_2][S]}{k_{-1} + k_3 [S]} + k_4 \left(\sqrt{\frac{k_2}{k_{-2}} [A_2]} \right) [S] \quad (8)$$

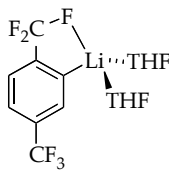
Part 5: Computational Studies



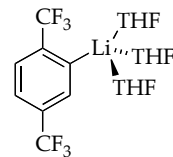
A



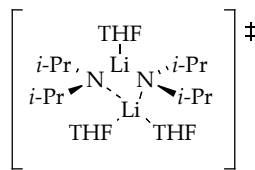
B



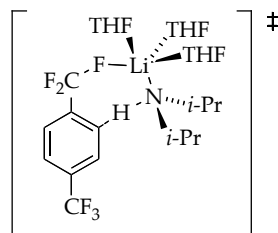
C



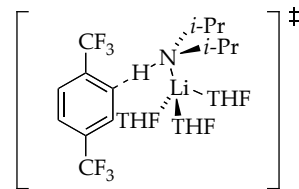
D



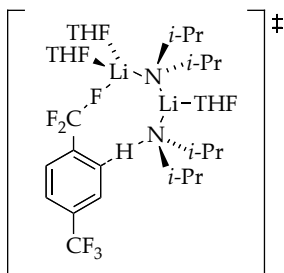
E



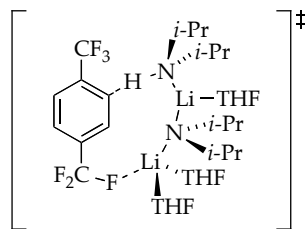
F



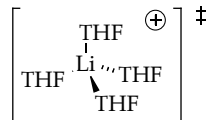
G



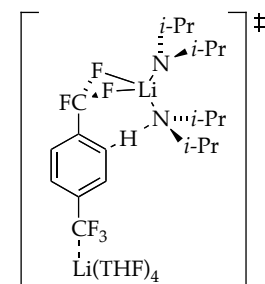
H



I

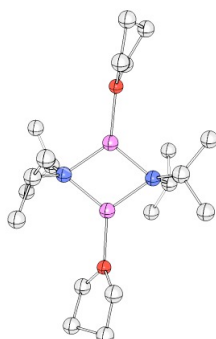
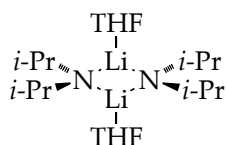


J



K

Table 1. Optimized geometries at B3LYP level of theory with 6-31G(d) basis set for the reactants at $-78\text{ }^\circ\text{C}$ with free energies (Hartrees) and cartesian coordinates (X, Y, Z) (Note: G_{MP2} includes single point MP2 corrections to B3LYP/6-31G(d) optimized structures).

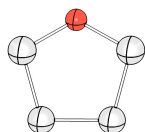
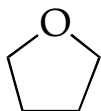


3
 $G = -1063.135501$
 $G_{\text{MP2}} = -1059.937725$

Atom	X	Y	Z	Atom	X	Y	Z
N	0	0	0	H	-0.940577	-3.291008	-1.825271
C	-0.215739	0.612452	1.318612	C	-2.275223	-4.680069	-0.904214
C	0.984066	1.381887	1.921761	H	-2.504256	-5.19534	-1.84738
H	1.212505	2.284952	1.34251	H	-2.310069	-5.431695	-0.105932
H	0.778689	1.697923	2.953722	H	-3.068237	-3.948858	-0.708955
H	1.882702	0.753584	1.932942	C	0.182248	-5.031842	-1.330903
C	-1.475882	1.513412	1.414833	H	0.292339	-5.788992	-0.544657
H	-1.662511	1.833942	2.448825	H	-0.066363	-5.560021	-2.261741
H	-1.371101	2.42064	0.807577	H	1.156355	-4.547171	-1.460089
H	-2.362674	0.977827	1.055352	O	2.890094	-2.114628	-0.276836
H	-0.400482	-0.231238	2.010144	C	3.52909	-2.599416	-1.47886
C	0.294364	0.950027	-1.075375	C	5.02417	-2.634817	-1.16185
H	-0.088612	1.959024	-0.838431	C	5.17113	-1.444535	-0.201398
C	1.804497	1.126678	-1.373756	C	3.871831	-1.516212	0.604784
H	1.981395	1.865835	-2.168777	H	3.498476	-0.537145	0.916021
H	2.34994	1.453509	-0.48314	H	3.974185	-2.15728	1.489104
H	2.239835	0.172163	-1.698457	H	5.220904	-0.505023	-0.763636
C	-0.411394	0.5173	-2.373716	H	6.058482	-1.507597	0.435346
H	-0.126925	-0.512599	-2.63791	H	5.642686	-2.546191	-2.059904
H	-1.500227	0.542654	-2.246722	H	5.286266	-3.571958	-0.656761
H	-0.152964	1.159869	-3.226138	H	3.104737	-3.577461	-1.718479
Li	-1.462938	-1.378687	-0.078227	H	3.309896	-1.905896	-2.301885
Li	0.922415	-1.791464	0.023104	O	-3.431996	-1.14847	-0.425881
N	-0.560416	-3.145972	0.199308	C	-4.064444	-1.141073	-1.728456
C	-0.522816	-3.873798	1.472891	C	-5.569847	-1.045588	-1.463002
H	-0.46329	-4.963706	1.307703	C	-5.702828	-1.732285	-0.094683
C	0.733203	-3.499287	2.286203	C	-4.431019	-1.269572	0.614429
H	0.750947	-2.417347	2.490329	H	-4.055787	-1.97603	1.358533
H	0.766551	-4.00792	3.259096	H	-4.566131	-0.288873	1.089082
H	1.643109	-3.758699	1.732093	H	-5.700242	-2.822319	-0.210242

Table 1 (Continued).

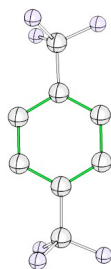
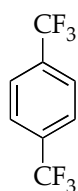
C	-1.771806	-3.638553	2.355096	H	-6.60968	-1.447449	0.44699
H	-1.728216	-4.20067	3.299517	H	-6.159851	-1.526531	-2.248671
H	-1.859018	-2.571836	2.60852	H	-5.883179	0.002828	-1.396109
H	-2.683407	-3.937095	1.82658	H	-3.667369	-0.297566	-2.299805
C	-0.893909	-3.980504	-0.960233	H	-3.802081	-2.073238	-2.243737



A
 $G = -232.349367$
 $G_{\text{MP2}} = -231.6694404$

Atom	X	Y	Z
C	0	0	0
O	1.132807	-0.739653	-0.442032
C	2.264796	-0.012388	0.019216
C	1.92285	1.47444	-0.210686
C	0.368847	1.489728	-0.185167
H	-0.032338	2.108191	0.623792
H	2.365524	2.11958	0.5546
H	2.296315	1.80941	-1.183111
H	2.436349	-0.210295	1.091379
H	3.13745	-0.361827	-0.539569
H	-0.860576	-0.323589	-0.591979
H	-0.206691	-0.218661	1.061467
H	-0.031366	1.878296	-1.126381

Table 1 (Continued).



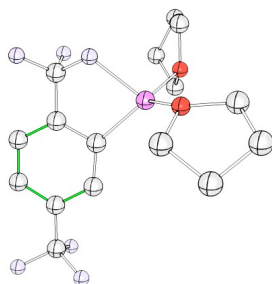
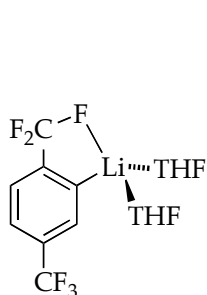
B

$G = -906.232925$

$G_{\text{MP2}} = -903.9700518$

Atom	X	Y	Z
C	0	0	0
C	-1.505925	0.032078	-0.000082
C	-2.199386	1.240823	-0.000053
C	-3.59506	1.240823	-0.000003
C	-4.288522	0.032078	0.000028
C	-3.591787	-1.182468	0.000001
C	-2.202658	-1.182468	-0.000058
H	-1.656905	-2.120819	-0.00011
H	-4.137541	-2.120819	0.000027
C	-5.794446	0	0.000016
F	-6.272325	-0.650206	-1.08545
F	-6.333334	1.236442	0.000523
F	-6.272317	-0.651108	1.084947
H	-4.139698	2.178082	0.000014
H	-1.654749	2.178082	-0.000084
F	0.477838	-0.649702	1.085789
F	0.477912	-0.651611	-1.084607
F	0.538888	1.236442	-0.001049

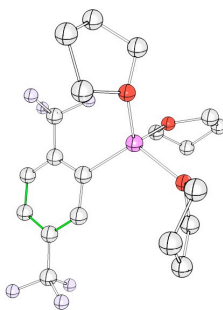
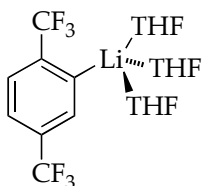
Table 2. Optimized geometries at B3LYP level of theory with 6-31G(d) basis set for the serial solvation of **C** and **D** at $-78\text{ }^{\circ}\text{C}$ with free energies (Hartrees) and cartesian coordinates (X, Y, Z) (Note: G_{MP2} includes single point MP2 corrections to B3LYP/6-31G(d) optimized structures).



C
 $G = -1377.907053$
 $G_{\text{MP2}} = -1374.2644$

Atom	X	Y	Z	Atom	X	Y	Z
C	0	0	0	H	-1.946008	-1.583823	-4.733239
C	1.201259	0.624969	-0.64827	H	-1.398545	-1.427745	-3.047946
C	0.980986	1.589795	-1.657516	H	-4.160658	-0.69365	-4.167982
C	2.174286	2.061903	-2.244922	H	-3.82412	-1.701574	-2.750382
C	3.44926	1.621147	-1.867383	H	-3.207441	0.203343	-1.412113
C	3.598932	0.666126	-0.856026	H	-4.308539	1.049445	-2.530166
C	2.460508	0.162205	-0.237549	O	-1.722611	3.803523	-1.16997
H	2.556523	-0.573166	0.557457	C	-2.691462	4.589891	-1.906131
H	4.586649	0.333843	-0.55483	C	-2.320081	6.062253	-1.668289
C	4.659727	2.143818	-2.588016	C	-0.835645	5.981499	-1.273899
F	5.801042	1.981985	-1.876064	C	-0.794145	4.678078	-0.482661
F	4.55392	3.465363	-2.870052	H	-1.135534	4.819212	0.551779
F	4.853472	1.515995	-3.776067	H	0.17629	4.176653	-0.480051
H	2.122353	2.817238	-3.029464	H	-0.49899	6.841469	-0.687676
Li	-1.039707	2.071383	-1.723567	H	-0.200497	5.901973	-2.163628
O	-2.282102	1.202371	-2.969336	H	-2.909378	6.477916	-0.843113
C	-3.406388	0.432491	-2.464248	H	-2.498726	6.680851	-2.552494
C	-3.476708	-0.837133	-3.323411	H	-2.618841	4.306236	-2.961904
C	-2.030186	-0.982434	-3.823317	H	-3.69479	4.339	-1.546078
C	-1.629531	0.472492	-4.042277	F	-0.418987	-1.137038	-0.621207
H	-1.994585	0.85701	-5.004514	F	0.17366	-0.320477	1.297214
H	-0.557482	0.662991	-3.952826	F	-1.109484	0.839294	-0.033341

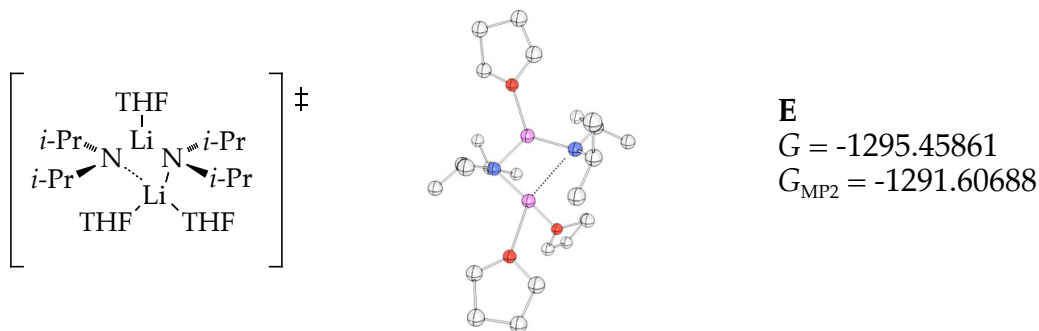
Table 2 (Continued).



D
 $G = -1610.253454$
 $G_{MP2} = -1605.959647$

Atom	X	Y	Z	Atom	X	Y	Z
C	0	0	0	F	0.366552	-0.618982	-1.166369
C	-1.280095	0.777744	-0.143239	F	1.069917	0.775586	0.340894
C	-1.211102	2.128546	-0.55715	O	0.339579	5.194262	-1.423521
C	-2.487721	2.708636	-0.73307	C	0.484322	5.563751	-2.803596
C	-3.696557	2.035062	-0.5222	C	-0.952682	5.685554	-3.308691
C	-3.693431	0.699423	-0.108648	C	-1.683865	6.30284	-2.093728
C	-2.470381	0.065916	0.078315	C	-0.764444	5.959471	-0.894181
H	-2.445976	-0.973508	0.395015	H	-1.245802	5.339894	-0.135117
H	-4.625732	0.168675	0.055219	H	-0.372807	6.867756	-0.416392
C	-4.998456	2.766185	-0.673877	H	-2.6887	5.889505	-1.972686
F	-4.93928	3.734505	-1.624208	H	-1.782451	7.387841	-2.201678
F	-5.371621	3.388616	0.475155	H	-1.35118	4.690086	-3.529119
F	-6.020569	1.944214	-1.01272	H	-1.03504	6.297717	-4.211896
H	-2.561209	3.743069	-1.064474	H	1.018373	6.524513	-2.874874
Li	0.604902	3.210493	-0.794735	H	1.082182	4.786869	-3.282257
O	1.659833	3.649597	0.878832	O	1.894954	2.578484	-2.221931
C	2.521817	4.797625	1.052279	C	3.208522	2.118959	-1.831193
C	2.442569	5.183512	2.540536	C	3.303627	0.683006	-2.340909
C	1.139185	4.509933	3.002199	C	2.500775	0.761753	-3.649281
C	1.132275	3.237774	2.159703	C	1.373769	1.73643	-3.287983
H	0.144681	2.81136	1.977896	H	0.489671	1.222757	-2.903315
H	1.782908	2.464669	2.591001	H	1.078644	2.381732	-4.122472
H	0.270945	5.13138	2.7531	H	2.113188	-0.208441	-3.972625
H	1.117101	4.306236	4.076968	H	3.12186	1.167148	-4.457056
H	2.444167	6.267652	2.687552	H	2.812253	0.004767	-1.63832
H	3.295827	4.771253	3.091028	H	4.33791	0.356232	-2.485954
H	3.539066	4.529773	0.742782	H	3.966036	2.764486	-2.298782
H	2.151686	5.584336	0.388546	H	3.279844	2.212835	-0.745077
F	-0.065379	-0.982949	0.930582				

Table 3. Optimized geometries of trisolvated LDA open dimer transition state structures at B3LYP level of theory with 6-31G(d) basis set for the ortholithiation of **1** at $-78\text{ }^{\circ}\text{C}$ with free energies (Hartrees), and cartesian coordinates (X,Y,Z). (Note: G_{MP2} includes single point MP2 corrections to B3LYP/6-31G(d) optimized structures)

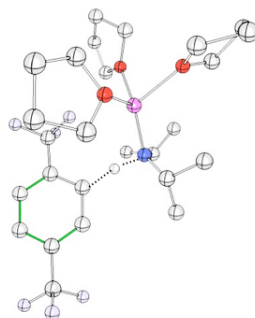
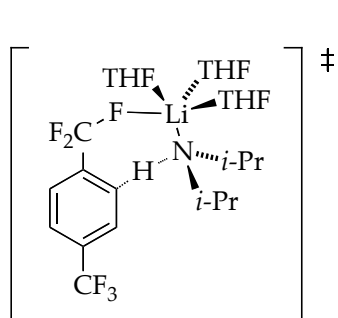


Atom	X	Y	Z	Atom	X	Y	Z
C	0	0	0	C	-0.297343	-2.91898	4.819492
N	0.330915	-0.051082	1.422569	C	1.039513	-3.303098	5.496281
Li	0.986676	-1.672013	2.368464	H	1.824191	-2.582994	5.228076
N	-0.282232	-2.951862	3.349522	H	0.942489	-3.302802	6.590401
Li	-1.64914	-1.778369	2.432447	H	1.383128	-4.300321	5.20026
O	-3.075329	-0.436062	2.943572	C	-0.708565	-1.534135	5.334881
C	-2.84135	0.979554	2.799132	H	-1.682181	-1.232428	4.935819
C	-3.092344	1.53698	4.198001	H	-0.777125	-1.528438	6.430134
C	-4.263684	0.664608	4.708739	H	0.02156	-0.770802	5.041526
C	-4.192193	-0.612199	3.833537	H	-1.051191	-3.623592	5.223685
H	-4.011404	-1.525555	4.405869	O	2.957949	-2.23587	2.144177
H	-5.108242	-0.747326	3.24293	C	3.839073	-1.579267	1.198093
H	-4.168411	0.434692	5.77365	C	5.260195	-1.938343	1.635383
H	-5.223512	1.171845	4.566428	C	5.060173	-3.329132	2.255506
H	-2.202051	1.391064	4.817817	C	3.712153	-3.165101	2.957009
H	-3.331755	2.60452	4.189773	H	3.13656	-4.089837	3.039553
H	-3.554451	1.39297	2.068543	H	3.834023	-2.738861	3.960801
H	-1.822166	1.077853	2.420136	H	4.995314	-4.092702	1.471043
O	-3.503113	-2.916608	1.39482	H	5.857543	-3.617842	2.947029
C	-4.012701	-4.255303	1.589486	H	5.966577	-1.930488	0.799832
C	-5.258243	-4.383549	0.701005	H	5.62115	-1.232105	2.392805
C	-5.715985	-2.924267	0.562604	H	3.624822	-0.508578	1.218396
C	-4.376772	-2.191292	0.507948	H	3.616782	-1.960727	0.195054
H	-3.959349	-2.201454	-0.508403	C	1.178976	1.079778	1.803019
H	-4.416882	-1.157824	0.857707	C	1.754242	0.887495	3.21633
H	-6.332889	-2.743613	-0.323031	H	2.356703	-0.026582	3.300152
H	-6.286983	-2.614417	1.446515	H	2.398485	1.728568	3.502729
H	-4.989408	-4.790007	-0.280963	H	0.941025	0.827574	3.950073
H	-6.016037	-5.03962	1.139706	C	0.502409	2.476781	1.767272
H	-4.255821	-4.377537	2.652162	H	-0.234466	2.572867	2.57531

Table 3 (Continued).

H	-3.230278	-4.974039	1.331682	H	1.243737	3.277433	1.899679
C	0.001158	-4.298846	2.83583	H	-0.011352	2.663144	0.818405
C	-0.899415	-5.428177	3.390368	H	2.059852	1.173151	1.125303
H	-1.959154	-5.177334	3.265482	C	-1.249688	-0.837808	-0.293613
H	-0.703634	-6.37467	2.869043	H	-2.109656	-0.454238	0.266453
H	-0.727917	-5.606058	4.457096	H	-1.511508	-0.825292	-1.360224
C	-0.071347	-4.303505	1.301159	H	-1.090417	-1.888183	-0.014883
H	0.615745	-3.568952	0.861903	C	1.138208	-0.456515	-0.947194
H	0.200404	-5.286148	0.894782	H	1.356435	-1.522714	-0.796038
H	-1.083814	-4.062232	0.954224	H	0.873604	-0.31234	-2.004863
H	1.037301	-4.618883	3.082845	H	2.059933	0.106639	-0.7627
H	-0.253896	1.030267	-0.31996				

Table 4. Optimized geometries of monomer-based transition state structures at B3LYP level of theory with 6-31G(d) basis set for the ortholithiation of **1** at $-78\text{ }^{\circ}\text{C}$ with free energies (Hartrees), and cartesian coordinates (X,Y,Z). (Note: G_{MP2} includes single point MP2 corrections to B3LYP/6-31G(d) optimized structures)

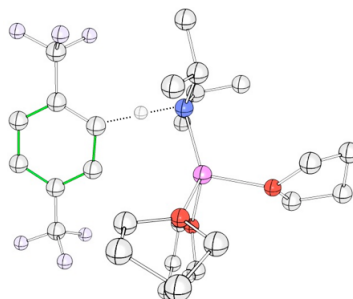
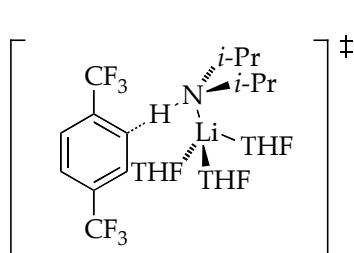


F
 $G = -1902.453745$
 $G_{\text{MP2}} = -1897.287936$

Atom	X	Y	Z	Atom	X	Y	Z
Li	0	0	0	H	-2.065919	-3.87235	0.249237
F	1.545013	-2.09467	-0.010064	H	-2.593875	-1.516035	0.69611
C	2.723025	-2.673943	-0.388153	H	-3.338613	-1.333845	-0.909359
C	3.906978	-1.770606	-0.195866	H	-1.050651	-1.817627	-2.908917
C	5.133265	-2.395836	0.077719	H	0.064761	-2.718598	-1.861065
C	6.276806	-1.624194	0.247653	H	1.636755	0.021042	-4.262057
C	6.171008	-0.236071	0.133428	C	1.84339	2.350617	-0.306742
C	4.936436	0.357531	-0.154422	H	2.327134	2.016377	0.626304
C	3.748312	-0.375753	-0.333723	C	2.87618	3.254637	-1.020872
H	4.912584	1.441363	-0.244333	H	2.421971	3.846778	-1.824528
C	7.372433	0.635132	0.37184	H	3.307515	3.965821	-0.305365
F	7.457279	1.642404	-0.528685	H	3.6956	2.675098	-1.456233
F	7.33528	1.220648	1.596325	C	0.651408	3.231442	0.121434
F	8.536185	-0.054922	0.307709	H	0.987217	4.053986	0.768433
H	7.232652	-2.088904	0.463375	H	0.157746	3.683874	-0.747932
H	5.195722	-3.476824	0.16629	H	-0.094603	2.647484	0.667591
F	2.810607	-3.82311	0.335151	O	0.324454	-0.524824	1.983782
F	2.540507	-3.05922	-1.680587	C	-0.268177	-1.710266	2.559288
N	1.487742	1.089421	-1.000472	C	0.590078	-2.06929	3.775015
C	1.297753	1.207803	-2.462595	C	1.973899	-1.555555	3.350874
H	1.880268	2.051607	-2.860747	C	1.621921	-0.276548	2.59299
C	-0.166418	1.465131	-2.874902	H	2.328146	-0.032984	1.797328
H	-0.550239	2.389694	-2.431494	H	1.523621	0.582052	3.270609
H	-0.26366	1.552554	-3.966217	H	2.460866	-2.272095	2.681522
H	-0.812579	0.640575	-2.545417	H	2.642942	-1.366444	4.195444
C	1.826433	-0.043229	-3.183113	H	0.571777	-3.141468	3.992304
H	2.903232	-0.160956	-3.031566	H	0.238197	-1.535417	4.665948
H	1.346088	-0.953502	-2.810677	H	-1.308448	-1.485874	2.818293
C	-0.965957	-2.386331	-1.976645	H	-0.253994	-2.507069	1.807293

Table 4 (Continued).

O	-1.258589	-1.505056	-0.859361	O	-1.915811	1.040077	0.64693
C	-2.551397	-1.85216	-0.339885	C	-2.251395	1.351956	2.017645
C	-2.645158	-3.362706	-0.529296	C	-3.246808	2.513593	1.959064
C	-1.985676	-3.544201	-1.908359	C	-3.944322	2.270102	0.612242
H	-2.73312	-3.448477	-2.703394	C	-2.783013	1.771554	-0.248234
H	-1.505688	-4.520148	-2.021936	H	-2.220461	2.606268	-0.682095
H	-3.673792	-3.734336	-0.491216	H	-3.083197	1.098015	-1.055564
H	-2.704385	0.462412	2.477073	H	-4.416227	3.166204	0.198499
H	-1.329398	1.585943	2.554625	H	-4.713757	1.494832	0.712145
H	2.538908	0.330746	-0.724475	H	-2.715507	3.472129	1.944093
H	-3.932756	2.518781	2.811489				



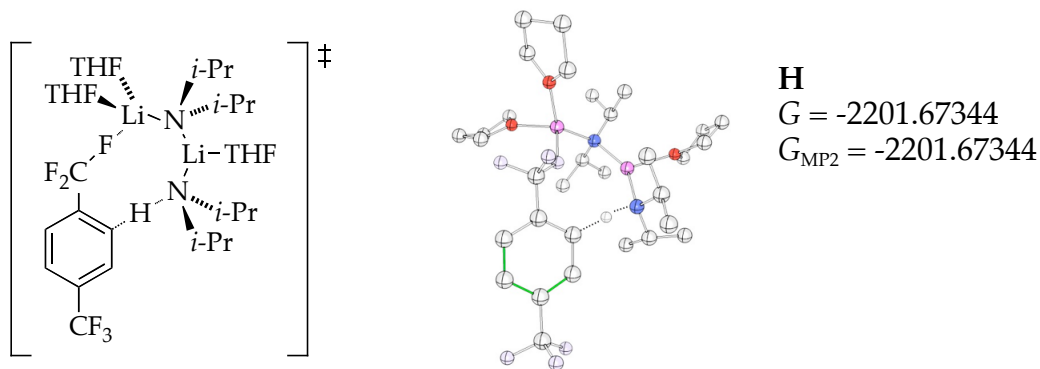
G
 $G = -1902.455318$
 $G_{\text{MP2}} = -1897.293589$

Atom	X	Y	Z	Atom	X	Y	Z
C	0	0	0	C	-3.876154	0.70273	-1.916701
C	0.299892	-1.463765	0.091404	C	-3.727669	-0.828191	-1.926217
C	1.61239	-1.918102	0.218953	H	-2.685986	-1.14084	-2.01999
C	1.838176	-3.29138	0.299153	H	-4.312059	-1.301821	-2.721891
C	0.757076	-4.179009	0.254859	H	-3.020908	1.19448	-2.387099
C	-0.587727	-3.76982	0.129538	H	-4.781677	1.007822	-2.453794
C	-0.761339	-2.380854	0.045402	H	-3.013453	1.099869	0.041254
H	-1.770573	-1.980281	-0.061676	H	-4.541185	1.966565	-0.230653
C	1.039161	-5.65517	0.357437	H	-5.828694	-0.105503	-0.087245
F	0.49165	-6.353938	-0.666461	H	-4.588237	-0.403013	1.159438
F	0.529871	-6.190681	1.501288	O	-3.980437	-2.428127	2.271635
F	2.363652	-5.949377	0.360663	C	-5.043221	-2.38179	3.246818
H	2.853442	-3.663817	0.392499	C	-4.489764	-1.571568	4.418367
H	2.440219	-1.218113	0.251439	C	-3.00529	-1.966497	4.396001
F	-0.669804	0.316756	-1.145341	C	-2.714079	-2.068574	2.89717
F	1.09754	0.782204	0.036763	H	-1.979431	-2.833065	2.639412
F	-0.81152	0.42245	1.018564	H	-2.385431	-1.113707	2.473685
H	-1.837801	-4.523642	0.028017	H	-2.862917	-2.938536	4.881931

Table 4 (Continued).

N	-3.060497	-4.991591	-0.1361	H	-2.356157	-1.240519	4.893923
Li	-4.152653	-3.271043	0.337674	H	-4.98974	-1.806802	5.362772
O	-6.221207	-3.47258	0.302631	H	-4.605115	-0.497467	4.229193
C	-7.017642	-2.991588	-0.807364	H	-5.920946	-1.937394	2.769265
C	-8.374835	-3.691416	-0.688942	H	-5.29178	-3.406774	3.555017
C	-8.002018	-5.010728	0.004644	C	-3.126924	-5.42712	-1.546554
C	-6.909467	-4.556565	0.971179	H	-2.341034	-6.175635	-1.748257
H	-6.173524	-5.329581	1.202617	C	-4.471962	-6.06225	-1.947182
H	-7.3379	-4.177402	1.909155	H	-4.460039	-6.36061	-3.003587
H	-7.594697	-5.724473	-0.719494	H	-4.71173	-6.953124	-1.35763
H	-8.844208	-5.484071	0.517978	H	-5.287907	-5.339995	-1.810399
H	-8.853807	-3.833704	-1.662058	C	-2.843254	-4.246362	-2.482095
H	-9.055571	-3.107342	-0.058211	H	-2.777546	-4.58577	-3.523432
H	-7.082745	-1.902486	-0.741097	H	-3.652461	-3.50707	-2.427902
H	-6.505035	-3.255885	-1.739625	H	-1.903486	-3.750518	-2.225313
O	-4.212397	-1.305235	-0.639795	C	-3.291935	-6.109047	0.812636
C	-4.747139	-0.190221	0.102434	C	-2.940285	-5.661986	2.239296
C	-4.001999	1.033193	-0.420801	H	-3.478314	-4.749375	2.512627
H	-1.464142	-7.28593	0.509809	H	-3.200524	-6.443564	2.963899
H	-2.785326	-8.167215	1.293849	H	-1.866419	-5.467211	2.325476
H	-2.833991	-7.870045	-0.4436	H	-4.368841	-6.370537	0.814995
C	-2.546347	-7.430239	0.51626				

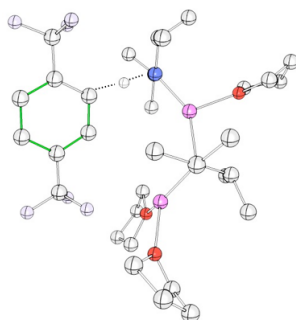
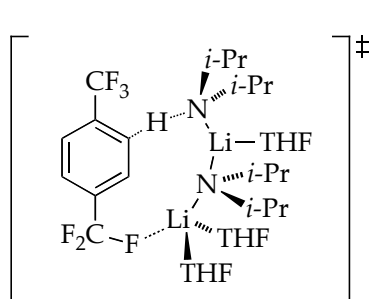
Table 5. Optimized geometries of dimer-based transition state structures at B3LYP level of theory with 6-31G(d) basis set for the ortholithiation of **1** at $-78\text{ }^{\circ}\text{C}$ with free energies (Hartrees), and cartesian coordinates (X,Y,Z). (Note: G_{MP2} includes single point MP2 corrections to B3LYP/6-31G(d) optimized structures)



Atom	X	Y	Z	Atom	X	Y	Z
Li	0	0	0	H	-0.337915	5.205289	1.975749
F	1.919926	0.280235	0.70689	H	0.521493	6.564748	1.219138
C	2.950701	-0.393385	1.332851	H	-2.442735	6.30198	1.614743
F	2.683518	-1.713842	1.15399	H	-1.50894	7.735416	1.183915
F	2.77314	-0.161539	2.660499	C	-1.758212	2.20445	-0.758713
C	4.297248	0.024467	0.830434	H	-1.925654	3.201641	-1.213265
C	4.512826	1.379568	0.513877	C	-2.879533	1.302861	-1.328505
C	5.83323	1.671754	0.118908	H	-2.81603	1.193555	-2.416481
C	6.84356	0.706861	0.043477	H	-2.834204	0.29691	-0.886219
C	6.573635	-0.626014	0.367997	H	-3.869019	1.721781	-1.102662
C	5.287676	-0.968792	0.76603	C	-2.009906	2.380516	0.745909
H	5.058998	-2.00034	1.018838	H	-1.253383	3.02728	1.202409
H	7.352179	-1.378307	0.301316	H	-2.992203	2.832959	0.933631
C	8.241702	1.110901	-0.334923	H	-1.982595	1.411721	1.258729
F	8.955395	0.077797	-0.846497	O	-0.738235	-0.708529	1.762689
F	8.255977	2.098939	-1.259042	C	-1.72433	-1.764999	1.823858
F	8.941182	1.571404	0.732371	C	-1.906844	-2.081642	3.309658
H	6.091672	2.693014	-0.15301	C	-1.617936	-0.722536	3.965052
N	-0.382466	1.730717	-0.98615	C	-0.482606	-0.187676	3.093868
C	-0.083729	1.530185	-2.415489	H	0.495515	-0.547374	3.425938
H	-0.790095	0.810105	-2.878385	H	-0.451839	0.902339	3.027136
C	-0.185188	2.796865	-3.297275	H	-1.331984	-0.800893	5.017984
H	0.025924	2.561882	-4.348686	H	-2.496087	-0.069712	3.896264
H	-1.185988	3.241237	-3.258377	H	-1.170908	-2.825751	3.636145
H	0.537713	3.559702	-2.977991	H	-2.905172	-2.469368	3.533059
C	1.311802	0.910113	-2.586781	H	-2.655895	-1.397913	1.372806
H	2.089267	1.538515	-2.140167	H	-1.357971	-2.608023	1.233588
H	1.368502	-0.075823	-2.112993	O	-0.141257	-1.826551	-1.001426

Table 5 (Continued).

H	1.555495	0.780663	-3.648856	C	0.862532	-2.876649	-0.99454
Li	0.947642	3.177182	-0.211144	C	0.405973	-3.910349	-2.029645
N	2.845883	3.604032	0.517146	C	-0.440419	-3.064496	-2.992743
C	3.655473	4.494704	-0.345689	C	-1.120928	-2.093783	-2.031855
H	4.707417	4.502858	-0.005585	H	-2.011417	-2.54564	-1.571629
C	3.205543	5.967879	-0.368617	H	-1.400433	-1.140335	-2.482103
H	3.302806	6.451187	0.609603	H	-1.157437	-3.653197	-3.572607
H	3.818943	6.541246	-1.075339	H	0.201324	-2.516617	-3.691985
H	2.158101	6.044801	-0.682421	H	-0.213339	-4.682708	-1.558162
C	3.667296	3.947748	-1.778389	H	1.250707	-4.406953	-2.515575
H	3.981278	2.90039	-1.80043	H	1.824557	-2.426879	-1.25926
H	2.669491	4.014418	-2.233046	H	0.936851	-3.279688	0.018769
H	4.355326	4.52249	-2.410854	H	3.561778	2.48217	0.539386
C	2.776665	4.080999	1.915761	H	4.664267	3.257608	2.668744
H	2.309383	5.079827	1.944998	O	-0.183386	5.09359	-0.065337
C	1.870586	3.153951	2.738974	C	-0.747256	5.870739	-1.131911
H	0.874429	3.055764	2.285471	H	-0.040653	6.662914	-1.424589
H	2.298271	2.152028	2.822439	H	-0.905914	5.204723	-1.979833
H	1.731518	3.546969	3.754319	C	-2.029614	6.459946	-0.538128
C	4.140554	4.218392	2.631635	H	-2.845405	5.736285	-0.629988
H	4.796221	4.936589	2.128065	H	-2.335211	7.382299	-1.041091
H	3.999734	4.572122	3.66133	C	-1.658319	6.676632	0.951228
C	-0.337462	5.888207	1.124165				



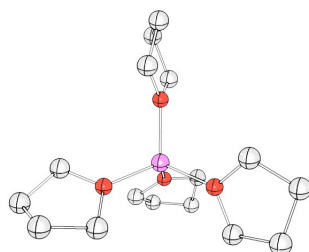
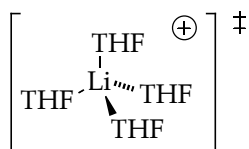
I
 $G = -2201.665013$
 $G_{\text{MP2}} = -2195.577105$

Atom	X	Y	Z	Atom	X	Y	Z
C	0	0	0	H	3.877434	9.389276	1.076968
C	1.45488	-0.106454	-0.314976	H	3.728451	7.130643	1.953243
C	2.283075	1.004956	-0.104262	H	5.410376	6.766986	1.493931
C	3.656507	1.004886	-0.37565	C	1.096047	4.878844	-2.392617
C	4.155455	-0.220953	-0.866264	H	0.058394	5.013884	-2.766662
C	3.356269	-1.351698	-1.07627	C	1.493029	3.436175	-2.738672

Table 5 (Continued).

C	1.991261	-1.298885	-0.802719	H	2.537983	3.236593	-2.479541
H	1.359245	-2.164531	-0.969415	H	0.893718	2.697974	-2.192503
H	3.791513	-2.270834	-1.455004	H	1.370486	3.238486	-3.811434
C	5.622704	-0.31785	-1.206594	C	1.960836	5.843186	-3.235463
F	6.417566	0.044824	-0.170401	H	1.833649	5.645928	-4.307913
F	5.959798	0.486542	-2.247455	H	1.699447	6.89244	-3.060703
F	6.002703	-1.573024	-1.55898	H	3.026555	5.718973	-3.002421
H	1.829702	1.921732	0.278045	C	0.805291	6.44371	-0.520689
F	-0.73192	-1.052509	-0.41364	H	1.565884	7.175689	-0.853084
F	-0.241246	0.142841	1.33454	C	0.779458	6.532147	1.012402
F	-0.567995	1.112685	-0.581934	H	0.652912	7.568618	1.350525
Li	-0.267534	3.807717	-0.268755	H	-0.049725	5.943129	1.427112
N	1.164378	5.073542	-0.931114	H	1.708878	6.148136	1.447619
Li	3.202842	4.834227	-0.342831	C	-0.541645	6.98541	-1.054374
N	4.721203	3.502482	0.147063	H	-1.37831	6.360687	-0.714347
C	5.031494	3.519378	1.592015	H	-0.719346	8.005258	-0.688899
C	3.723318	3.457083	2.392253	H	-0.575013	7.019117	-2.148218
H	3.042427	4.272061	2.111337	O	-0.856115	3.334818	1.569641
H	3.204041	2.508907	2.214483	C	-2.149335	2.743598	1.86469
H	3.914463	3.542602	3.469449	C	-2.031187	2.128458	3.263336
H	5.51577	4.475727	1.85977	C	-0.909468	2.962646	3.901455
C	5.977441	2.398971	2.079262	C	0.022239	3.185188	2.714645
H	5.558389	1.41035	1.87135	H	0.674707	2.321375	2.549948
H	6.955441	2.449383	1.590307	H	0.631067	4.087811	2.783559
H	6.144929	2.485145	3.161028	H	-0.410795	2.452589	4.730733
C	5.927866	3.56161	-0.708933	H	-1.297388	3.919965	4.269719
C	6.890857	4.723074	-0.403556	H	-1.727994	1.079935	3.188536
H	6.37445	5.686169	-0.489351	H	-2.974544	2.175944	3.815348
H	7.321169	4.658207	0.601661	H	-2.897534	3.544473	1.835556
H	7.726961	4.719023	-1.114616	H	-2.378503	2.011921	1.087935
C	5.494286	3.628712	-2.178311	O	-2.036453	3.591229	-1.312058
H	4.818395	2.805908	-2.423884	C	-2.213477	2.863092	-2.544546
H	4.981826	4.577115	-2.395678	C	-3.056461	3.784468	-3.445277
H	6.360883	3.560066	-2.847422	C	-3.749598	4.75372	-2.447786
H	6.512082	2.631992	-0.602417	C	-3.293688	4.243078	-1.07254
O	4.035292	6.813113	-0.063624	H	-4.00572	3.512283	-0.66098
C	4.505509	7.315642	1.206517	H	-3.128265	5.030418	-0.334497
C	4.79607	8.79885	0.97939	H	-4.839791	4.747815	-2.537648
C	5.285082	8.798712	-0.476696	H	-3.40506	5.779424	-2.604968
C	4.386795	7.73764	-1.120142	H	-3.774229	3.209344	-4.037402
H	4.883692	7.179064	-1.918709	H	-2.417974	4.336826	-4.139799
H	3.462627	8.172941	-1.518273	H	-1.223659	2.635447	-2.93814
H	6.336353	8.49223	-0.524254	H	-2.736364	1.922103	-2.326677
H	5.192882	9.772467	-0.967024	H	4.266891	2.291101	-0.111196
H	5.533457	9.193231	1.684997				

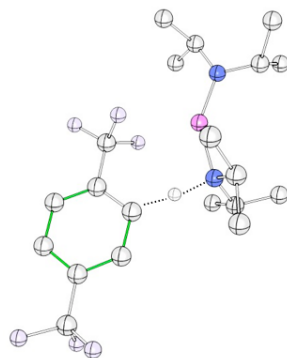
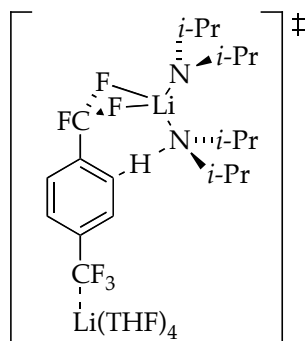
Table 5 (Continued).



J
 $G = -936.851978$
 $G_{\text{MP2}} = -934.1446904$

Atom	X	Y	Z	Atom	X	Y	Z
Li	0	0	0	H	-2.149322	1.360014	1.952391
O	-1.144662	0.198341	-1.583784	H	-3.126007	0.082431	1.188036
C	-2.266027	-0.669753	-1.889826	H	-2.244754	0.281713	4.111398
C	-3.233358	0.194136	-2.694152	H	-3.817297	-0.240458	3.486664
C	-2.268198	1.082764	-3.494689	H	-2.023838	-2.161565	4.219983
C	-1.137065	1.33501	-2.49278	H	-2.868102	-2.359883	2.674355
H	-1.30352	2.242085	-1.901185	H	-0.574485	-2.37367	1.87507
H	-0.150424	1.395803	-2.96245	H	-0.061385	-1.22254	3.136545
H	-2.726206	2.012594	-3.841897	O	1.248352	-1.490122	-0.303631
H	-1.89292	0.543866	-4.371491	C	2.438788	-1.778754	0.478115
H	-3.853719	0.800389	-2.024102	C	2.9693	-3.112277	-0.049936
H	-3.89651	-0.40046	-3.328057	C	2.528907	-3.075513	-1.521572
H	-1.90499	-1.524549	-2.476451	C	1.157422	-2.409918	-1.426419
H	-2.66937	-1.036861	-0.942332	H	0.367328	-3.141381	-1.214007
O	1.004177	1.651159	0.331102	H	0.877839	-1.832653	-2.311274
C	2.164628	2.100408	-0.420458	H	2.478552	-4.066127	-1.981308
C	2.491539	3.495199	0.113757	H	3.214918	-2.459861	-2.114295
C	2.016898	3.403227	1.572368	H	2.493874	-3.95013	0.472418
C	0.753912	2.554012	1.442173	H	4.051254	-3.206039	0.075205
H	-0.122744	3.168683	1.200723	H	3.159331	-0.966262	0.324596
H	0.531655	1.947891	2.32427	H	2.156801	-1.804335	1.534784
H	1.816528	4.378903	2.022881	O	-1.139352	-0.408864	1.552755
H	2.762987	2.889887	2.189439	C	-0.883468	-1.508994	2.467919
H	1.921633	4.258314	-0.427999	C	-2.186969	-1.711595	3.237157
H	3.553779	3.735711	0.019551	C	-2.739125	-0.279391	3.310447
H	2.985022	1.394472	-0.243293	C	-2.355933	0.285873	1.942054
H	1.910857	2.08539	-1.48443				

Table 5 (Continued).



K
 $G = -1497.09314$
 $G_{\text{MP2}} = -1493.001723$
 (calculation does not
 include $\text{Li}(\text{THF})_4^+$ ion)

Atom	X	Y	Z	Atom	X	Y	Z
C	0	0	0	H	11.869147	0.149489	1.115158
C	1.37859	-0.58757	-0.073634	H	11.763527	1.878075	0.740327
C	2.502526	0.249372	-0.07264	H	10.596947	1.129298	1.862021
C	3.815766	-0.24614	-0.079696	C	10.991792	0.577622	-1.557262
C	3.920775	-1.648893	-0.08613	H	11.701643	-0.260434	-1.553977
C	2.818612	-2.513172	-0.094385	H	10.304347	0.428791	-2.39813
C	1.533936	-1.977789	-0.084975	H	11.570579	1.496359	-1.739515
H	0.664859	-2.627958	-0.093795	C	6.100362	2.141097	-1.280174
H	2.956811	-3.590439	-0.108066	H	6.951439	2.844865	-1.264132
C	5.305462	-2.236455	-0.111286	C	6.352763	1.178761	-2.451157
F	5.32963	-3.582354	0.019637	H	5.55363	0.432536	-2.522283
F	5.976209	-1.944282	-1.257829	H	6.397944	1.723023	-3.403969
F	6.093909	-1.740705	0.897038	H	7.30271	0.64581	-2.322263
H	4.96277	0.595538	-0.06902	C	4.836196	2.986227	-1.56524
H	2.338913	1.326666	-0.075554	H	3.953571	2.344291	-1.67179
F	-0.940054	-0.804523	-0.562904	H	4.634133	3.704031	-0.761625
F	-0.404406	0.208886	1.281758	H	4.95209	3.558953	-2.49573
F	-0.088015	1.198922	-0.623912	C	5.920008	2.193611	1.186005
N	6.055363	1.372312	-0.025767	H	4.955325	2.742634	1.192054
Li	7.48032	-0.073043	0.09975	C	7.026662	3.251654	1.360545
N	9.306302	-0.475242	0.022407	H	6.906699	3.782378	2.31517
C	9.965188	-1.766056	0.121444	H	8.015134	2.774941	1.35358
H	11.06769	-1.662229	0.147091	H	7.011244	4.00396	0.564005
C	9.578846	-2.497941	1.426328	C	5.897955	1.27057	2.414947
H	9.867157	-1.896318	2.295918	H	5.71417	1.845585	3.332358
H	8.491415	-2.640393	1.467823	H	5.114158	0.512818	2.322655
H	10.052734	-3.48879	1.511682	H	6.860573	0.753657	2.531229
C	9.649665	-2.683818	-1.086716	H	10.138918	-3.669072	-1.01235
H	8.566362	-2.844622	-1.158118	C	10.191982	0.648356	-0.227765
H	9.971194	-2.209695	-2.020718	H	9.542522	1.536408	-0.323471
C	11.165948	0.974363	0.938045				

References

1. *Gaussian 09*, Revision A.1, Frisch, M. J.; Trucks, G. W.; Schlegel, H. B.; Scuseria, G. E.; Robb, M. A.; Cheeseman, J. R.; Scalmani, G.; Barone, V.; Mennucci, B.; Petersson, G. A.; Nakatsuji, H.; Caricato, M.; Li, X.; Hratchian, H. P.; Izmaylov, A. F.; Bloino, J.; Zheng, G.; Sonnenberg, J. L.; Hada, M.; Ehara, M.; Toyota, K.; Fukuda, R.; Hasegawa, J.; Ishida, M.; Nakajima, T.; Honda, Y.; Kitao, O.; Nakai, H.; Vreven, T.; Montgomery, Jr., J. A.; Peralta, J. E.; Ogliaro, F.; Bearpark, M.; Heyd, J. J.; Brothers, E.; Kudin, K. N.; Staroverov, V. N.; Kobayashi, R.; Normand, J.; Raghavachari, K.; Rendell, A.; Burant, J. C.; Iyengar, S. S.; Tomasi, J.; Cossi, M.; Rega, N.; Millam, N. J.; Klene, M.; Knox, J. E.; Cross, J. B.; Bakken, V.; Adamo, C.; Jaramillo, J.; Gomperts, R.; Stratmann, R. E.; Yazyev, O.; Austin, A. J.; Cammi, R.; Pomelli, C.; Ochterski, J. W.; Martin, R. L.; Morokuma, K.; Zakrzewski, V. G.; Voth, G. A.; Salvador, P.; Dannenberg, J. J.; Dapprich, S.; Daniels, A. D.; Farkas, Ö.; Foresman, J. B.; Ortiz, J. V.; Cioslowski, J.; Fox, D. J. Gaussian, Inc., Wallingford CT, 2009.
2. *Gaussview*, Version 3.09, Dennington 2, R.; Keith, T.; Millam, J.; Eppinett, K.; Hovell, W. L.; Gilliland, R.; Semichem, Inc.; Shawnee Mission, KS, 2003.